POUNDING CONTROL DESIGN OF ELEVATED BRIDGES UNDER SEISMIC EXICATION

A Thesis

Submitted in partial fulfillment of the requirements for the award of the degree of

MASTER OF TECHNOLOGY

IN

CIVIL ENGINEERING

With specialization in

STRUCTURE ENGINEERING

Under the supervision of

Mr. Chandra Pal Gautam

(Assistant Professor)

By

Rohit Sharma
(162663)

To

JAYPEE UNIVERSITY OF INFORMATION TECHNOLOGY

WAKNAGHAT, SOLAN – 173234

HIMACHAL PRADESH, INDIA

May, 2018

CERTIFICATE

This is to certify that the work which is being presented in the project entitled **"POUNDING CONTROL DESIGN OF ELEVATED BRIDGES UNDER SEISMIC EXICATION"** in partial fulfilment of the requirements for the award of the degree of Master of technology in Structrure Engineering and submitted to Department of Civil Engineering, Jaypee University of Information Technology, Waknaghat is an authentic record of work carried out by **Rohit Sharma** during a period from August 2017 to May 2018 under the supervision of **Mr. Chandra Pal Gautam** (Assistant Professor), Civil Engineering Department, Jaypee University of Information Technology, Waknaghat.

The above statement made is correct to the best of my knowledge.

Date: -

Dr. Ashok Kumar Gupta
Professor and Head of Department

External Examiner

Mr. Chandra Pal Gautam
(Supervisor)
Assistant Professor

ABSTRACT

Pounding during sever earthquakes can result in catastrophic structural damage in adjacent superstructure segments in elevated bridge.. Pounding may yield detrimental forces that could result in large displacement of deck and potential catastrophe of bridge. Past many earthquakes have done sever damage to bridges due to pounding. Aim of this thesis is to analyse pounding between superstructure segments of an elevated bridge induced by seismic waves. In this thesis a 3D model of a bridge is modelled in CSI Bridge software. In the model we provide expansion joint at every span of bridge. When bridge was analysed in software found that there was very high axial force, moment, stress, displacement in that bridge.

So to overcome that forces another model has been created. In this model lead rubber bearing has provide at every expansion joint and this result in decreasing in forces. But the forces were still very high. Than rubber isolator was introduced at expansion joints. This results in decreasing in large displacement and axial force. Than model forces were improved by introducing high damping rubber bearing in expansion joint. All the four models high damping rubber bearing has very high stiffness to reduce pounding force. So in this thesis we were able to reduce pounding forces by providing best suited material properties in expansion joint.

Keywords: *Pounding, Expansion joints, Lead rubber bearing, rubber isolator, High damping rubber bearing, stiffness.*

ACKNOWLEDGEMENT

I would like to express my profound sense of deepest gratitude to my guide and motivator Mr. Chandra Pal Gautam(Assistant Professor) Department of Civil Engineering, Jaypee University of Information Technology, Waknaghat, Distt. Solan, for their valuable guidance and co-operation for providing necessary facilities and sources during the entire period of this project. I would like to express my gratitude to Mr. Chandra Pal Gautam (Assistant Professor**)** for helping me in learning CSI Bridge software. I wish to convey my sincere gratitude to all the faculties of Civil Engineering Department who have enlightened me during my studies. The facilities and co-operation received from the technical staff of Department of Civil Engineering is thankfully acknowledged. I would like to thank my parents for their continuous support and help in achieving my goals.

ROHIT SHARMA

(162663)

TABLE OF CONTANTS

LIST OF TABLES

TABLE NO. **PAGE NO.**

LIST OF FIGURES

FIGURE NO. **PAGE NO.**

LIST OF SYMBOLS

NAME	SYMBOL
Lumped mass	Mi
Stiffness of element	Ki
Damping of element	Ci
Damping ratio	ξ

Chapter 1
INTRODUCTION

1.1 General

Multispan highway bridges are very common in India. During the earthquake bridge suffers severe damage due to collision between deck and abutment and between deck to deck collisions. Pounding between two deck portions are usually seen in past seismic earthquakes. Nearby building endures exceptionally serious harm amid seismic earthquake because of impact. All in all most regular approach to abstain from pounding of bridges is to give expansive joint between neighbouring portions. After the Kobe earthquake in japan seismic disconnection of bridges turned out to be extremely well known. According to earthquake design code expansion joint should be large adequate to evade crash however than expanding expansion joints is not a desired solution and it is very costly.

1.2 Pounding

Pounding happens when seismic uprooting surpasses the clear distance between neighbouring span which results in pounding. Pounding for the most part happens at joint area where expansion joints are given. Pounding may go from minor harm at area level for e.g. Concrete smashing, shear key harm, abutment tilting etc. and real harm at worldwide level for e.g. Span unseating. Ponding in bridges might be unavoidable where typical thermal expansion joints are provided and can turn out to be extremely more serious issue where very large displacements are expected. Figure 1, shows the damage on bridge due to pounding.

1.3 Damage due to pounding

1.3.1Area Damage:-

1. Concrete smashing
2. Shear key harm
3. Abutment tilting

1.3.2 Worldwide damage:-

1. Span unseating
2. Bridge fall

Figure1: Damage due to pounding of bridge

1.4 Pounding in bridge deck

Pounding in bridge may occur due to the collision of two head-to-head decks. It needs high bearing expansion joint to provide stiffness to the bridge. For bridges which have high isolation properties requires ratio of natural frequency of piers to deck greater than 10. Due to this response obtain from the piers are very less so we can ignore this in study of pounding. For batter explanation we can treat every structure segment as single degree of freedom which have mass Mi. lumped mass is mounted on a spring Dashpot system which syndicates all the factors of bearing which supports the section ki" + k", ci" + c"

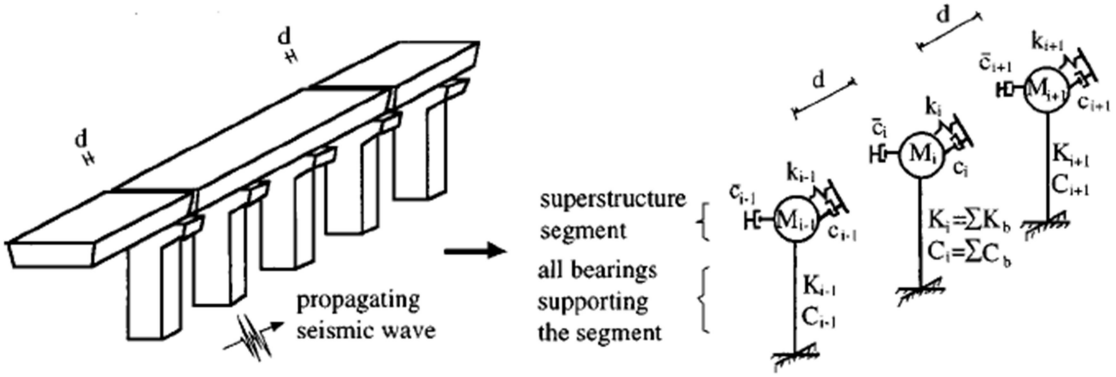

Figure: 2 simple model of pounding

When a bridge segment collides they form a very complicated process due to this a multi-dimensional process forms. When collision happens it results in very large axial forces

in bridge. Also very large transverse forces generated due to transverse motion of bridge deck. But it has found that transvers forces are very much lesser than longitudinal forces so we can assume that there will be no displacement in transverse direction thus this assumption is used in pounding. Modelling of collision is done by impact viscoelastic element. Pounding occurs when relative displacement is much higher than gap between decks. To elaborate pounding problem we can create two sets of diffential equation. When two decks moves towards each other it forms 1st set and 2nd set occurs there is contact between them. These changes in stages pretend the boundary non linearity.

Damping, stiffness and mass of impact element can be calculate by formula given below.

$$Ci = 2\xi\sqrt{ki\frac{Mi}{2}} \qquad \text{eq. a}$$

Where Ci is damping coefficient, Mi is lumped mass, Ki is stiffness and ξ is damping ratio. Damping ratio may range from 0.5 to 0.75 to describe real collision [14].

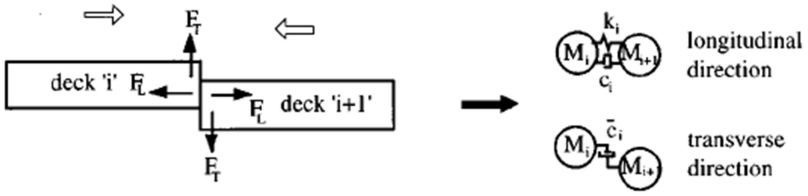

Figure 3: Model of collision of bridge deck

1.5 Equation of motion of bridge

$$\begin{bmatrix} M & 0 \\ 0 & M \end{bmatrix}\begin{bmatrix} \ddot{x(t)} \\ \ddot{y(t)} \end{bmatrix} + \begin{bmatrix} C(t) & 0 \\ 0 & \overline{C(t)} \end{bmatrix}\begin{bmatrix} \dot{x(t)} \\ \dot{y(t)} \end{bmatrix} + \begin{bmatrix} K(t) & 0 \\ 0 & \overline{K} \end{bmatrix}\begin{bmatrix} x(t) \\ y(t) \end{bmatrix}\begin{bmatrix} D(t) \\ 0 \end{bmatrix} = -\begin{bmatrix} M & 0 \\ 0 & M \end{bmatrix}\begin{bmatrix} \ddot{xg(t)} \\ \ddot{yg(t)} \end{bmatrix} \qquad \text{eq.b}$$

1.6 Methods of seismic analysis

When bridge comes under seismic excitation this can only be analysed by analytic methods. These analytic methods are elastic in nature and can also be non-elastic in nature. Seismic analysis of any structure can be done by liner or nonlinear static and dynamic analysis

1.6.1 Static linear analysis

Static linear analysis says that when we apply a fixed load on the bridge. It will always be remain in elastic form. Static analysis is very less complex method of analysis a bridge. The load applied on the bridge will be equal to inertia force which relates the mode of vibration. A response which is inelastic in nature can be represented by inertia force. When earth moves due to earthquake a flexible response my results in plastic hinge. The method of analysis may accept that real quality of bridge is bigger than the plan quality. This can dissipate energy through yielding.

1.6.2 Dynamic linear analysis

It is conventional method. It can also be used as spectrum analysis or it can be used as time history analysis. It is mostly used to calculate the response generated by moving loads. It is very common method to calculate response of bridge.

1.6.3 Response spectrum analysis

It is used to find the response of bridge from the modal frequency.it represents the most extreme response of the structure. It provides the understanding of displacement and velocity of an structure which has damping. It is viable to envelope response spectra with the end goal that a smooth bend speaks to the pinnacle response for every acknowledgment of auxiliary period.

Response-spectrum analysis is helpful for design since it relates basic compose determination to dynamic execution. Structures of shorter period encounter more prominent increasing acceleration, while those of longer period encounter more displacement. Basic execution targets ought to be considered amid preparatory design and response-spectrum analysis.

1.7 Methods to overcome pounding

Pounding can be overcome by following methods

1. Pounding can be reduce by increasing clear distance between two head to head decks. But there is limitation in increasing the gap between decks
2. Pounding can be reduce by providing high stiffness bearing at expansion joint location.

3. Pounding can also be reduce by providing stiff connection to the deck so that bridge can move as whole structure.

1.8 Importance of study

Bridges are very important structure. These are lifelines off any road grid system. These structures are very important for the betterment and development of mankind. Before 2000 all bridges were designed only to with stand vehicle loads. But these bridges were helpless under earthquakes. As the time progress need of change in design procedure of bridges also changes which helps in introducing new techniques for design of bridge. During earth quake bridge suffers sever damage due to pounding of bridge. For the construction of bridge requires lots of time and money but when bridge damaged due to earthquake it require more money for repairing work. So it is important to introduce some design technique to reduce pounding of bridges. In this thesis work a concrete bridge is analysed and some material has introduced to overcome pounding.

1.9 Organization of thesis

Chapter 1 comprises introduction to pounding in elevated bridges and importance, objective and scope of the research.

Chapter 2 comprises the literature review of past research papers on the analysis of bridges.

Chapter 3 comprises the modelling of the bridge, using CSI Bridge software.

Chapter 4 comprises Analysis and Results

Chapter 5 comprises comparison of results

Chapter 6 includes conclusion of thesis

Chapter 2
LITRATURE REVIEW

2.1 General

To deliver a comprehensive review of literature related to pounding control design of elevated bridge. For starting a thesis there are many good references from where we can start our work. This literature review is focused on pounding of bridges, methods to overcome pounding, effects of pounding on bridges, methods of analysis of bridge etc.

Amjadian, M., & Agrawal, A. K. [1] In this paper "Rigid-Body Motion of Horizontally Curved Bridges Subjected to Earthquake-Induced Pounding" a 3DOF model had been created for examine impact due to pounding on unbending frame movement of on a level plane curved bridges amid solid ground movements. Biaxial hysteresis demonstrates has been created for the cooperation of spiral and azimuthal shear power of section with a seismic tremor. Finite element investigation for model level curved bridge has been finished. A finite element examination had been performed on models of a Prototype Bridge by changing distinctive boundaries of bridges containing size of hole amongst deck and projections, subtended angle of the deck and grating coefficient. Aftereffect of the investigation demonstrates that spiral and azimuthal displacement and pivot of deck have increment with diminish in size of hole amongst deck and projections. Azimuthal displacement of outside section of the deck is by and large higher than those of inside segments. Characteristic time of the first and second hub diminishes with increment in shape of the deck. Pinnacle outspread displacement of corners of the deck amid pounding increments with diminishes in size of hole for all estimations of subtended angle.

The biggest spiral displacement happens of bridges with having subtended angle in scope of 45 to 900 and also hole size of 2.5 to 20 cm when there is no pounding. Pinnacle azimuthal displacement of corners of deck amid pounding increments with diminish in size of hole for subtended angle higher than 300 and reduction of subtended angle lower than 300. The biggest azimuthal displacement happens of bridges with subtended angle in scope of 90 to 1350 and hole size of 2.5 to 20 cm when there in pounding. AASHTO particular proposal demonstrating standard curved bridges with subtended angles under 90 by an identical straight bridge. Numerical outcome demonstrates that these proposals are not substantial when there is pounding a direct result of totally unique inflexible body movements of curved

and straight bridges amid pounding. The impact of grating on the pinnacle outspread displacement of corners of the deck for the most part relies upon the ground movement time history. Grating builds pivot of deck of curved bridges with a reduction in subtended angle for all hole measure when subtended angle is under 450. It ought to be noticed that these outcomes are constrained to cement to solid erosion.

Won, J. H., Mha, H. S., & Kim, S. H. [2] The earthquake-instigated pounding consequences for bridge piers are explored by examining dynamic reactions of a three-traverse principally upheld steel brace bridge. Utilizing a disentangled and glorified systematic model reflecting arbitrary attributes of seismic excitations, most extreme dock reactions are assessed. The nonlinear practices of strengthened solid docks and pounding between adjoining bridge decks are incorporated into the expository model by using a nonlinear hysteresis show and an effect component (a straight viscoelastic model), individually.

From the aftereffects of time history examination, it is discovered that pounding between nearby vibration units decreases the wharf powers and displacements by confining the dock movements. As the pinnacle ground speeding up builds, the consequences of the case without thought of pounding demonstrates the unfeasibly extensive dock displacements in the hysteresis display by overlooking limitation of wharf movements because of pounding. The outcomes as indicated by the hole separate between affect components demonstrate that the span of hole remove is vigorously connected to the nonlinear wharf practices. Along these lines, the impacts of pounding and nonlinear dock practices ought to be viewed as together to mirror the bridge reactions effectively.

Shrestha, B., Hao, H., & Bi, K. [3] Pounding harms to bridge had been seen in the past significant earthquakes. Late examinations had featured that modifying central times of contiguous basic components near each other, the main strategy recommended by the codes to alleviate pounding and unseating harm, isn't adequate to counteract such harms attributable to the relative displacement actuated by spatially changing ground movements. As pounding and unseating harm could prompt noteworthy loss of economy and life inferable from powerlessness to rapidly get to the harmed region instantly after an earthquake, it is vital to secure help bridge structures. Past earthquakes had uncovered that the normally utilized steel link restrainers had constrained adequacy. Moreover, just constrained research had concentrated on alleviating pounding powers on bridge joints which prompt restricted harms and disturbances of the serviceability of the bridge after solid shakings.

This examination introduces a broad examination on the adequacy of joining elastic bumpers as a stun engrossing gadget alongside Shape Memory Alloy (SMA) or steel link restrainers to relieve pounding and unseating harms on numerous traverse bridges endangered to spatially shifting ground movements. The reactions on bridge structures with various limiting gadgets acting alone and in mix with elastic bumpers subjected spatially shifting ground movements are thought about and talked about. The outcome shows that SMA restrainers joined with elastic bumpers can prompt better execution as far as diminishment of joint opening and moderation of vast pounding force..

Huo, Y., & Zhang, J. [4] In this paper Effects of Pounding and Skewness on Seismic Responses of Typical Multispan Highway Bridges Using the Fragility Function Method Fragility work technique is utilized to discover the pounding and Skewness of seismic conduct of run of the mill multispan RCC Bridge. 3D models are worked for run of the mill three traverse RCC bridge. The likelihood of Skewness and pounding harm in RCC Bridge are figured based on delicacy work technique. Here delicacy work technique is determined utilizing Probabilistic seismic request investigation PSDA or Increment Dynamic Analysis IDA.

Three models on the premise bridge model are fabricated. At that point a no. of earthquake records is utilized to discover the bridge reaction. Time History Analysis was performed on different bridge models. Delicacy examination is performed to discover the impact of pounding and Skewness on the bridges. Aftereffect of this paper demonstrate that for bridges without pounding (e.g. constant bridges and solid projections) connects with a coupled reaction of bridges and has less harm of wharfs and segments. To control pounding in straight bridges 8 cm hole estimate is sufficient and for skewed bridges 16 cm measure is adequate.

Dimitrakopoulos, E. G. [5] Point of this paper Seismic reaction examination of skew bridges with pounding deck– projection joints is to characterize the physical system if contact-actuated coupling between skew bridges between deck projection joints. In this paper a completely non-smooth approach is proposed. A skew bridge is broke down under basic heartbeat ground movement. In the wake of breaking down it has discovered that the skew bridge has inclination to transverse displacement and turn after deck projection impact isn't a factor of the skew angle alone but instead of the aggregate geometry in design in addition to erosion. Examination additionally demonstrates that coupling is more in low scope of

recurrence range where contact is more exceptional and regular. A pilot utilization of skew bridge is proposed. Investigation demonstrates that reaction pivot emerging from contact takes after the comparable example with proposed spectra and scale well with persistency of genuine earthquakes.

Wang, T. L., & Li, Q. N. [6] Point of this paper Effect of Expansion Joint on Seismic Response of Curved Ramp Bridge is to decide the impact of extension joints on seismic reaction of curved incline bridge. In this paper dynamic model of curved slope bridge with extension joints was manufactured. At that point nonlinear time history investigation was performed on four distinct models to fine the impact of seismic reaction on development joints under various seismic sources of info. ANSYS programming is utilized to perform limited component examination and nonlinear time history investigation on different models. Consequence of this examination demonstrates that for keep up uniform mass and solidness all through the structure a consistent support unit ought to be utilized. By crossing out the extension joints at projection are valuable to lessen pounding reaction of the bridges and to limit the seismic reaction of different segments.

Meng, Q., & Xia, Y. [7] In this paper, Seismic Pounding effect in Bridges with High Piers So as to think about the seismic pounding of high-dock bridges in the rugged regions of Chinese Western zone, a fiber component model of a bridge was set up, and the GAP cells were intercalated in expansion joints between principle bridge and approach bridge in high-piers bridges, trailed by a examination of its regular vibration attributes. Moreover, by investigation and examination, the seismic pounding reaction and its impacts on the bridge were talked about under Different earthquake movement. The investigation comes about demonstrate that seismic pounding impact was connected with normal time of bridge's each part and inputted earthquake movement's trademark, and can be useful in the bridge, to some degree.

Wang, J. W., Li, J. Z., & Fan, L. C. [8] In this paper Current Studies on Seismic Pounding Effect between Adjacent Bridge Decks and Falling-off Prevention Measures the current advancement of the seismic pounding impact between contiguous bridge decks and tumbling off measures were presented. Right off the bat, the registering hypotheses and expository strategies for contact-pounding between nearby bridge decks were introduced. Besides, the cutting edge of the hypothetical and trial contemplates on pounding impacts between nearby bridge decks subjected to longitudinal earthquake was inspected and abridged. In conclusion,

for measures of relieving pounding between nearby bridge decks, plan techniques for pivot situate width at extension joints, outline strategies for longitudinal restrainers and outline strategy for transverse shear keys were presented in the light of draw off-and-drop crumple of bridge decks amid earthquake; and pivot situate widths in the seismic determinations of various nations were investigations..

Soyluk, K. [9] Aim of this paper "Comparison of random vibration methods for multi-support Seismic excitation analysis of long-span bridges" is to find the spatial variability effects of ground motion on dynamic behavior of long span bridges. In this paper random vibration method and two responses spectrum method is uses to find the response. Random vibration method analysis is performed on the two deck type arch bridge and a cable stayed bridge model. Depending on the recording of ChiChi, Taiwan earthquake Power spectral density function is used in random vibration analysis.

In this paper Filtered White Noise Ground movements was utilized rather than genuine ground movement in light of the fact that after examination it has discovered that the both give same outcome. Because of correlation of recurrence area ghostly examination and reaction ghastly investigation for the two strategies the power unearthly thickness capacities are equivalent. Subsequently it has been discovered that for same ground movement distinctive arbitrary vibration strategies can cause altogether different outcomes which are reliant on the force and recurrence substance of energy phantom thickness work.

Kim, S. H., & Shinozuka, M. [10] This paper shows the aftereffect of an examination on the impact of pounding at development joints on solid bridge reaction to earthquake ground movements. A building approach, instead of continuum mechanics approach, is underscored. In the first place, the dynamic conduct of a damped multidegree-of-flexibility bridge framework isolated by an extension joint including an effect is inspected by methods for the limited component technique. Second, the affectability examination of the solidness in hole components is performed. Third, helpfulness of the examination technique for recreation of pounding wonders is exhibited and the impact of pounding on the malleability requests estimated as far as the turn of segment closes is explored. Two-dimensional limited component investigation utilizing a bilinear hysterestic show for bridge substructure joints and a nonlinear hole component for the extension joint is performed on a practical bridge with a development joint.

The impacts of the essential factors on the flexibility request, for example, hole sizes and qualities of earthquake ground movement are explored through a parametric report. The real conclusions are the impact of effect most straightforwardly relies upon the span of energy or pounding extent and the pounding impact is by and large observed to be immaterial on the malleability interest for wide viable scopes of hole size and pinnacle ground increasing speed, however is possibly critical at the areas of effect.

DesRoches, R., & Muthukumar, S. [11] In this paper "Impact of pounding and restrainers on seismic reaction of numerous edge bridges" Pounding between adjoining outlines in a various edge bridge produces bothersome powers bringing about substantial displacements, neighborhood harm, and conceivable disappointment of segment bents. In this investigation, explanatory models are utilized to analyze the variables influencing the worldwide reaction of a numerous edge bridge because of pounding of contiguous edges. Parameter investigations of uneven and two-sided pounding are directed to decide the impacts of edge solidness proportion, ground movement qualities, outline yielding, and restrainers on the pounding reaction of bridge outlines.

It is resolved that the most imperative parameters are the edge time frame proportion and the trademark time of the ground movement. The intensification in the edge reaction because of uneven pounding is most extreme for cases with exceedingly out-of-stage outlines, specifically for brief period structures. Two-sided pounding opens up the firm casing reaction, and decreases the adaptable casing reaction. The expansion of retainers minorly affects the uneven pounding reaction of very out-of-stage outlines. Current suggestions by Caltrans for constraints in outline period proportions to decrease the impacts of pounding are assessed.

Jankowski, R., Wilde, K., & Fujino, Y. [12] Aim of this paper Reduction of pounding impacts in lifted bridges amid Earthquakes is to break down a few techniques for diminishment of negative impacts of pounding by seismic waves. A n 3D basic model of a disengaged interstate bridge is presented. Impact of pounding is more longitudinal way and it likewise relies on the hole measure. After a point by point contemplate it has been discovered that for vast hole estimate are sufficient to counteract pounding and for little hole measure littlest reaction is acquired however these are not attractive arrangements.

Manual of Menshin Design of Highway Bridges is utilized to contemplate for the investigation a 3D shaft segment model and 3D spring dashpots are utilized. A SHOCK

TRANSMISSION UNIT is acquainted with abstain from pounding. Strategies presented in this paper are Gap estimate between the fragments, Rubber Bearing, Dampers and Stiffeners, Rubber guards, Crushable Devices, A nitty gritty examination of various techniques for decrease of pounding impacts has done in this paper. The aftereffect of this paper demonstrates that by putting hard elastic guards between bridge decks and by solid connecting the portions with each other adequately can successfully enhance the bridge conduct. So an exploratory outcome application STU can likewise be utilized for connecting the portions one with another. Additionally research should be possible to expand the information about the impact of pounding for various bridge structures

Kim, S. H., Lee, S. W., Won, J. H., & Mha, H. S. [13] A romanticized mechanical framework is proposed to look at the reaction practices of the bridge framework comprising of a few basic ranges. The framework is demonstrated as the numerous oscillators, and individual swaying units are made out of 3 level of-flexibility framework, which are translational movement of superstructure, and translational and rotational movements of establishments. The relating conditions of movement are then determined and the impacts of pounding and restrainers are broke down. The pounding is found to influence the worldwide movement of the bridge. It is discovered that the pounding may increment or decline the relative movements between neighboring units as indicated by the given conditions. The most extreme relative displacements happen between the projection and adjacent support. The restrainers are found to decrease the relative displacements proficiently bringing down the likelihood of traverse disappointments.

It is discovered that the proposed examination demonstrate utilizing the rearranged different oscillators is proper to assess the reaction practices of the few straightforward traverse bridge framework under seismic excitations uncovering the impacts of both pounding and restrainers. Utilizing the proposed framework, it is discovered that the pounding wonders can happen notwithstanding for the bridge framework comprising of the same wavering units, which have a similar characteristic frequencies. The pounding happens because of the higher solidness of the projection, and the connections are exchanged to the entire framework. It is discovered that the relative displacements in the centre segment of the bridge can be acquired, which can't be open without considering pounding.

Jankowski, R., Wilde, K., & Fujino, Y. [14] In this paper "pounding of superstructure fragments in disengaged raised bridge amid earthquakes" examination of pounding between

two bridge sections has been finished by seismic wave engendering. High damping elastic bearing gadget was proposed and essentialness of bearing was demonstrated. Super structure portion was dealt with as the one degree flexibility framework with lumped mass demonstrated on the spring mass damper framework. In this paper a strain rate subordinate model of high damping elastic bearing was proposed. Solidness and damping computed was Ki = 3.4751 x 109 ci = 1.8081 x 107. In this paper the investigation is planned for longitudinal and transverse movement of bridge deck. The consequence of this investigation shows that the crash has extensive effect on the structure conduct longitudinal way.

The investigation demonstrates that the reaction of the bridge depends the hole measure between the bridge decks. However, the impacts are as yet watched for vast upon holes. Consequence of the investigation additionally demonstrates that conduct of the bridge likewise relied upon the clear seismic speed. In this paper it has been demonstrated that to abstain from pounding a vast size hole between superstructures may be required and the response powers can be diminished by little holes by permitting pounding. Additionally research should be possible for more total and complex models, for example, non-direct reaction under expansive stacking and communication between piers establishment and soil.

Malhotra, P. K. [15] this paper manages collinear effect between solid poles of a similar cross segment however extraordinary lengths. It is demonstrated that the coefficient of compensation between bars depends just on the length proportion and the damping proportion of the bar material and the term of effect is equivalent to the basic time of pivotal vibration of the shorter bar. These outcomes are then utilized as a part of the second piece of this paper to department a sensible yet basic investigation of seismic pounding in solid bridges. In deciding a reasonable estimation of the coefficient of compensation, utilize is made of the solid movement information recorded on a solid bridge that accomplished critical pounding amid late California earthquakes. It is demonstrated that seismic pounding for the most part diminishes the section powers substantial effect powers produced in the superstructure are not transmitted to the bridge segments and establishments; and pounding does not build the longitudinal partition at the pivots.

The power of effect is specifically relative to the pressure wave speed and the approach speed of the two bars previously affect. Its size isn't truly influenced by material damping. A lot of vitality is lost by the proliferation of pressure waves produced by impacts. The rate of vitality misfortune increments with increment in the damping proportion and

lessens with increment in the length of the poles. The net vitality misfortune increments with increment in the proportion between the length of the more drawn out pole to that of the shorter pole. The impact of damping on the net vitality misfortune is most critical when the two bars are of a similar length. The coefficient of compensation is resolved exceptionally from the damping proportion and the length proportion of the two bars. The dominant part of force exchange between the bars happens over a term equivalent to the key time of hub vibration of the shorter pole. As it were, affect term is equivalent to double the time it takes the pressure wave to movement one finish length of the shorter bar.

2.2 Objective of study

1. To analyze a bridge model for without using stiffness in expansion joint.
2. To analyze a bridge model using lead rubber bearing, rubber isolator, high damping rubber bearing at gap location.
3. Compare the result to reduce pounding at gap location

2.3 Scope of study

The present investigation is constrained to those viable cases that go over in an elevated bridge. Currently the bridges are necessary due to new railroad projects in the country. It is absolutely necessary to bring the well-developed knowledge of the engineers on Highway Bridge to Railway Bridge engineering because Bridge needs careful design and detailing. An assortment of loads can be connected to a structure in the meantime. For instance a bridge may encounter dead load, live load, seismic load all the while. The objective of the thesis is to provide the bridge engineers with auxiliary manual material consists of comparison of load types as well as load combinations between highway and railway bridges as a quick reference in the process of design. The important parameters that will be considered in this study are:

Effect produced by pounding force on bridges.

Material use to overcome effect of pounding.

Compare the result to reduce pounding at gap location.

Chapter 3
BRIDGE MODELING IN CSI BRIDGE

3.1 General

CSI Bridge is design based software which allows designers to do simple analysis and modeling of bridges. Any types of bridges like concrete bridge, steel bridge, suspension or cable Stay Bridge and elevated bridges can be modelled in this software. This allows engineers to do modeling, designing and optimization of bridges very easily. CSI Bridge is very easy and friendly software for designing of a bridge.

CSI Bridge enables designers to assign bridge components which are already in the software. CSI Bridge account for dynamic effects, geometric nonlinearity and elastic and inelastic behaviour. It executes a parametric based demonstrating approach when creating explanatory frame work. It enables designers to assign bridge composition as an assembly of objects. CSI Bridge software automaticity assigns the material properties and does meshing for analysis.

CSI Bridge also allows importing files from Dxf/Dwg, IGES, CSI/2 and XML, which makes this software very user friendly. Different load cases like vehicle, seismic and wind can be created using AASHTO LFRD and IRC 6 design codes.

3.2 Bridge models

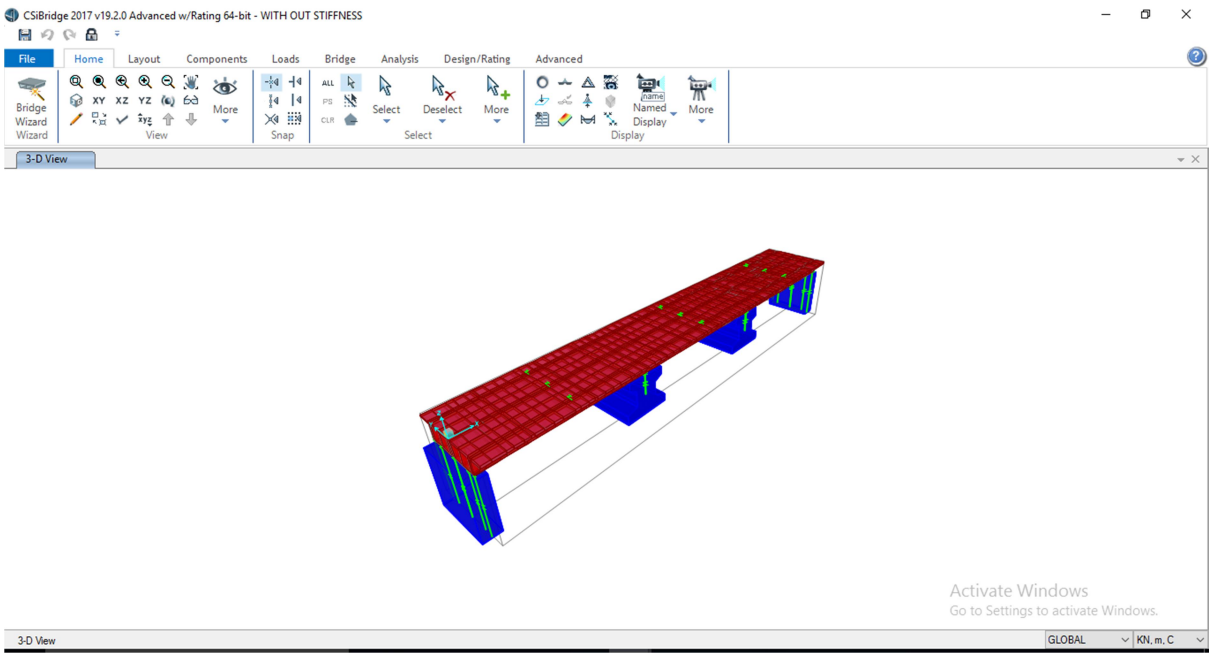

Figure 4 : Model 1 without stiffness in expansion joint

In fig. 4 expansion joints are provided at location 10m, 30m and 50m from starting point of bridge. In model 1no stiffness was provided to expansion joints due to this decks can easily collides with each other and creates high amount of pounding force.

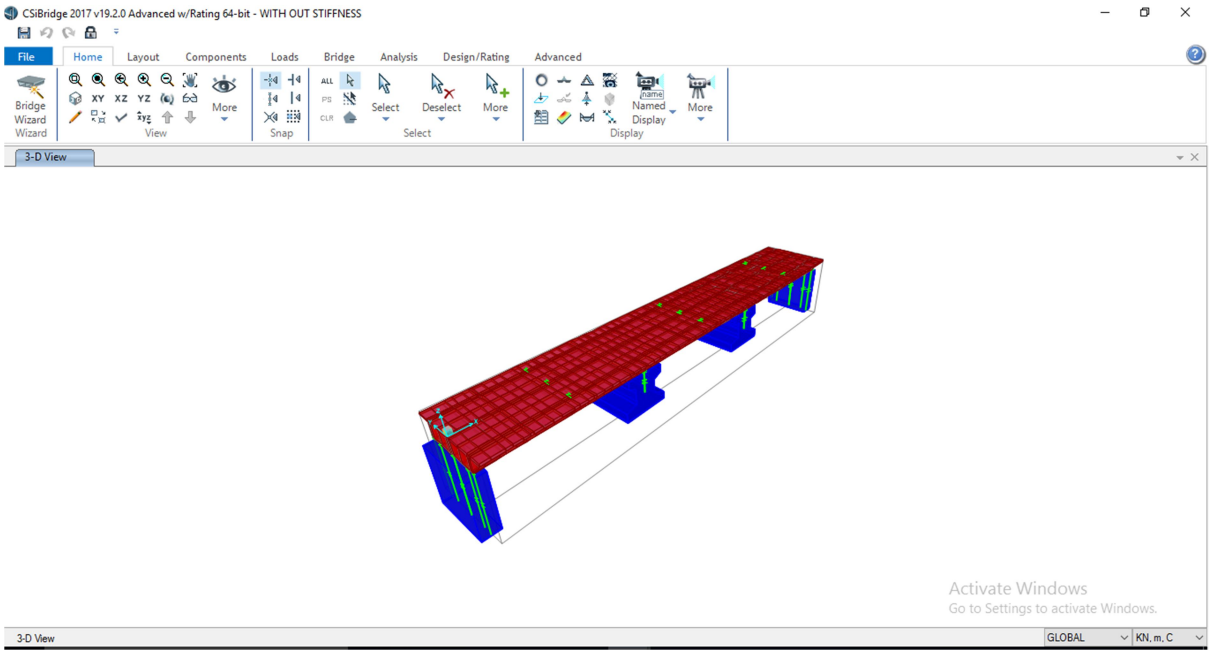

Figure 5: Model 2 Lead rubber bearing in expansion joint

In fig.5 model 2 was created using lead rubber bearing stiffness in expansion joint so that it can counter pounding force. Effective stiffness 2.097643 x 10^7 KN/m is used in modeling of lead rubber bearing.

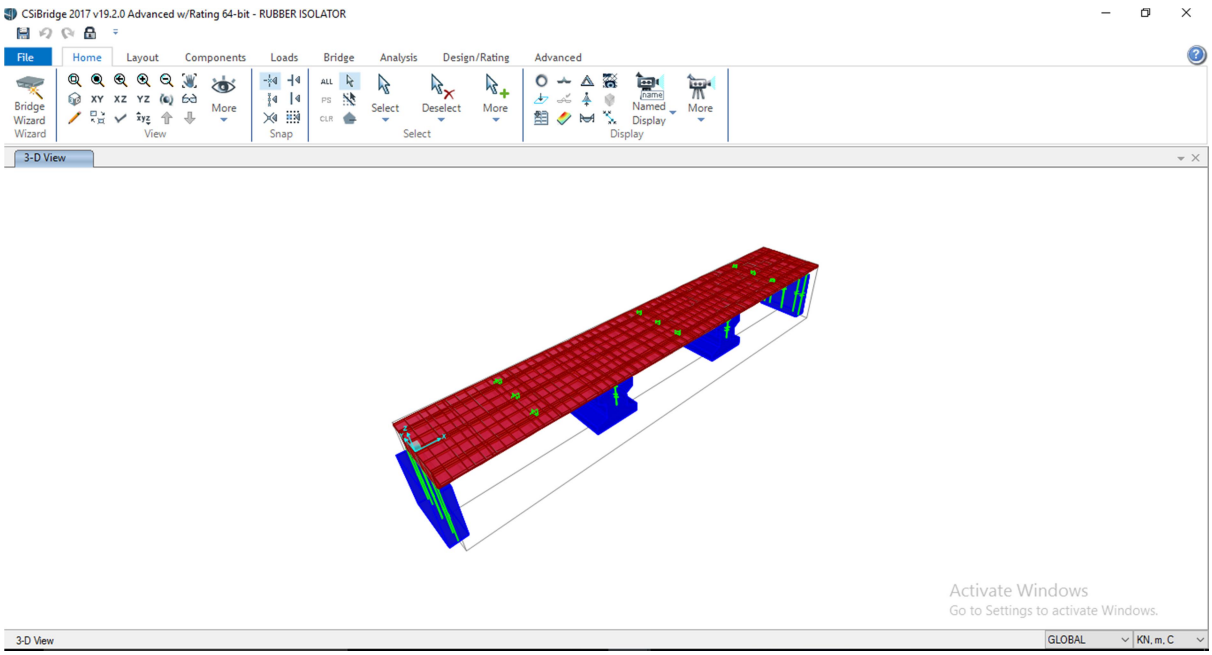

Figure 6: Model 3 Rubber isolator in expansion joint

In fig. 6 model 3 was created using rubber isolator stiffness in expansion joint so that it can counter pounding force. Effective stiffness 1.500 x 10^7 KN/m is used in modeling of rubber isolator bearing.

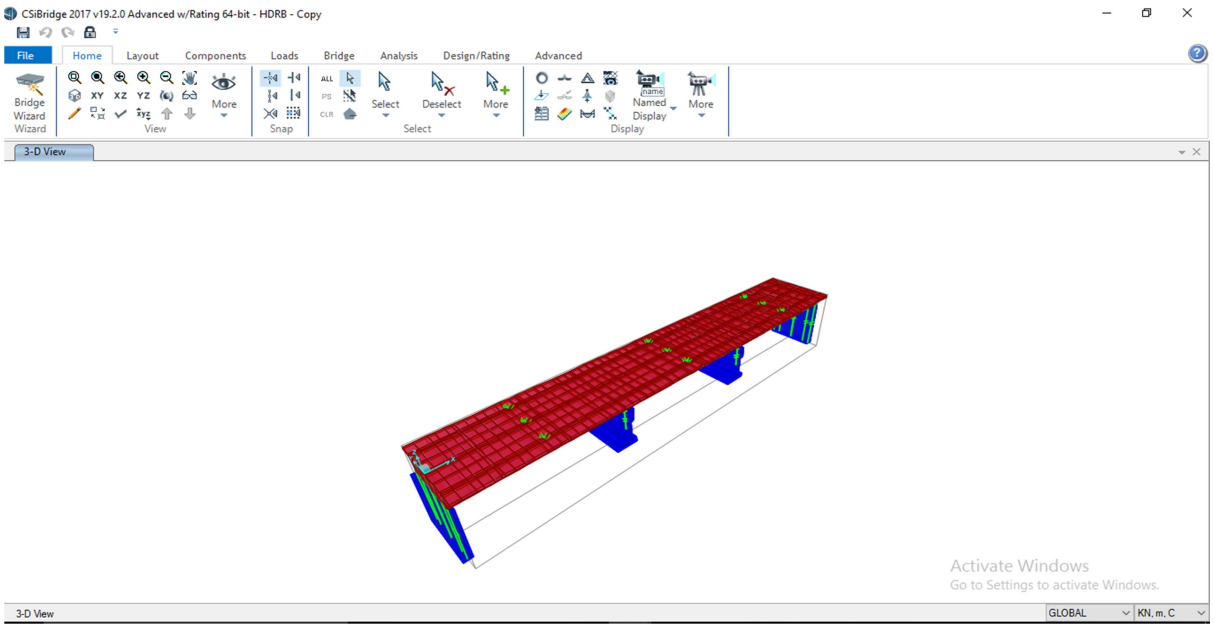

Figure 7: Model 4 High Damping Rubber Bearing in expansion joint

In fig. 7 model 4 was created using high damping rubber bearing stiffness in expansion joint so that it can counter pounding force. Effective stiffness 7.99 x 10^7 KN/m is used in modeling of high damping rubber bearing.

3.3 Bridge Layout

- No. of span – 3
- Span distance – 20m each
- Total length of span – 60m
- No. of lanes – 2

Table 1 : Lane data

Lane	Lane From	Layout Line	Station	Width	Offset
			M	m	M
LANE1	Layout Line	BLL1	0.	3.7	-1.85
LANE1	Layout Line	BLL1	60.	3.7	-1.85
LANE2	Layout Line	BLL1	0.	1.5	-4.45
LANE2	Layout Line	BLL1	60.	1.5	-4.45
LANE3	Layout Line	BLL1	0.	3.7	1.85
LANE3	Layout Line	BLL1	60.	3.7	1.85
LANE4	Layout Line	BLL1	0.	1.5	4.45
LANE4	Layout Line	BLL1	60.	1.5	4.45

Bridge component:

Properties of bridge components are shown in table 2-4

- Material properties: M30 concrete
- Deck section: Box girder
- Piers
- Abutment

1. **Deck section**

Table 2 : Deck section properties

No. of girder	1
Total width	10m
Total height	2m
Top slab thickness	0.25m
Bottom slab thickness	0.25m
Fillet horizontal dimension	0.15m
Fillet vertical dimension	0.15m
Material property	M30
Girder modelling type	Mixed

2. Piers

Table 3 : Pire section properties

Total width	5m
Total height	5m
Top slab thickness	0.5m
Bottom slab thickness	0.5m
Material property	M30
Girder modelling type	Mixed

3. Abutment

Table 4 : Abutment section properties

Total width	2m
Total height	7m
Material property	M30

4. Bearing

Table 5 : Bearing properties

Station	**Type**	**Bearing**	**Bearing Property**	**Bearing Elevation**
m				m
0.	Abutment	1	FIXED SUPPORT	-1.8288
0.	Abutment	2	FIXED SUPPORT	-1.8288
0.	Abutment	3	FIXED SUPPORT	-1.8288
10.	Hinge	1	EXPENSION JOINT	0.15
10.	Hinge	2	EXPENSION JOINT	0.15
10.	Hinge	3	EXPENSION JOINT	0.15
20.	Bent	1	FIXED SUPPORT	-1.8288
20.	Bent	2	FIXED SUPPORT	-1.8288
20.	Bent	3	FIXED SUPPORT	-1.8288
30.	Hinge	1	EXPENSION JOINT	0.15
30.	Hinge	2	EXPENSION JOINT	0.15
30.	Hinge	3	EXPENSION JOINT	0.15
40.	Bent	1	FIXED SUPPORT	-1.8288
40.	Bent	2	FIXED SUPPORT	-1.8288
40.	Bent	3	FIXED SUPPORT	-1.8288
50.	Hinge	1	EXPENSION JOINT	0.15
50.	Hinge	2	EXPENSION JOINT	0.15
50.	Hinge	3	EXPENSION JOINT	0.15
60.	Abutment	1	FIXED SUPPORT	-1.8288
60.	Abutment	2	FIXED SUPPORT	-1.8288
60.	Abutment	3	FIXED SUPPORT	-1.8288

3.4 Bridge Loading

In this bridge loading is taken as per IRC-6 design code. Dead load, IRC vehicle class –AA wheeled, class-A, wearing load, footpath load and railing load are assigned on bridge using load tab in csi bridge software. Earthquake load are assign as per IS 1893:2002 in x and y directions. All the load patterns used in modelling are given in table 6.

Table 6 : Bridge loading

Load Pattern	Design Type	Self-Weight	Auto Load
DEAD	Dead	1.	
CLASS-AA WHEELED	Vehicle Live	0.	
CLASS-A	Vehicle Live	0.	
EQ-X	Quake	0.	IS1893 2002
EQ-Y	Quake	0.	IS1893 2002
WEARING	Wearing Surface	0.	
FOOTPATH	Pedestrian LL	0.	
RAILING	Dead Manufacture	0.	

3.4.1 Railing Load

Railing load is applied in left and right lane of the bridge. The value of railing load as per IRC- 6 is 4 Kn/m. Railing load applied in csi bridge is given in table 7.

Table 7 : Railing load

Name	Type	Coordinate System	Direction	Reference Location	Distance	Load
					m	KN/m
RAILING RIGHT	Force	GLOBAL	Gravity	Right Edge of Deck	0.	4.
RAILING LEFT	Force	GLOBAL	Gravity	Left Edge of Deck	0.	4.

3.4.2 Footpath and Asphalt load

Footpath and Asphalt loads are applied at 8.5m and 1.5m respectively distance from the right edge of bridge. The value off footpath and asphalt load is 2 and 4.1 Kn/m^2 as per IRC-6 is shown in table 7.

Table 8 : Footpath and asphalt load

Name	Distance Right	Load left	Load right
	M	KN/m2	KN/m2
ASHPHALT	1.5	2.	2.
FOOTPATH LEFT	0.	4.1	0.
FOOTPATH RIGHT	8.5	0.	4.1

3.4.3 Vehicle Load

As per IRC-6 standard specification for vehicle load is given. Load pattern for vehicle loading was define in csi bridge software in the load tab. Axle width is taken as 1.8 m. Vehicle load applied for bridge is given in table 9.

Table 9 : Vehicle load

Vehicle Name	Load Type	Load	Type	Width	Axle Load	Axle Type	Axle Width	Min Distance
		KN/m		m	KN		m	m
IRC A	Leading Load	0.	Fixed Width	1.	26.478	Two Points	1.8	
IRC A	Fixed Length	0.	Fixed Width	1.	26.478	Two Points	1.8	1.1
IRC A	Fixed Length	0.	Fixed Width	1.	111.796	Two Points	1.8	3.2
IRC A	Fixed Length	0.	Fixed Width	1.	111.796	Two Points	1.8	1.2
IRC A	Fixed Length	0.	Fixed Width	1.	66.685	Two Points	1.8	4.3
IRC A	Fixed Length	0.	Fixed Width	1.	66.685	Two Points	1.8	3.
IRC A	Fixed Length	0.	Fixed Width	1.	66.685	Two Points	1.8	3.
IRC A	Fixed Length	0.	Fixed Width	1.	66.685	Two Points	1.8	3.
IRC A	Trailing Load	0.	Zero Width					
IRC AA Wheeled	Leading Load	0.	Fixed Width	1.	196.133	Fixed Width Line	2.5	
IRC AA Wheeled	Fixed Length	0.	Fixed Width	1.	196.133	Fixed Width Line	2.5	1.2
IRC AA	Trailing Load	0.	Zero Width					

Wheeled								
IRC AA Tracked	Leading Load	0.	Fixed Width	1.	0.	One Point		
IRC AA Tracked	Fixed Length	190.68	Fixed Width	2.9	0.	Fixed Width Line	1.	3.6
IRC AA Tracked	Trailing Load	0.	Fixed Width	2.9				
IRC 70R 7x2x2	Leading Load	0.	Fixed Width	1.	78.453	Two Points	1.94	
IRC 70R 7x2x2	Fixed Length	0.	Fixed Width	1.	117.68	Two Points	1.94	3.96
IRC 70R 7x2x2	Fixed Length	0.	Fixed Width	1.	117.68	Two Points	1.94	1.52
IRC 70R 7x2x2	Fixed Length	0.	Fixed Width	1.	166.713	Two Points	1.94	2.13
IRC 70R 7x2x2	Fixed Length	0.	Fixed Width	1.	166.713	Two Points	1.94	1.37
IRC 70R 7x2x2	Fixed Length	0.	Fixed Width	1.	166.713	Two Points	1.94	3.05
IRC 70R 7x2x2	Fixed Length	0.	Fixed Width	1.	166.713	Two Points	1.94	1.37

3.4.4 Seismic Loading as per IS 1893:2002

Response spectrum analysis is being done for bridge as per IS 1893: 2002. Analysis is done for zone 5 and soil type II. Modal damping is taken as 0.05. Earthquake loading is applied in both x and y direction. Load pattern, direction, zone code and soil type is given in table 10 and 11.

Table 10 : Seismic loading as per IS 1893: 2002

Load Pattern	Direction	Per cent	Ct	Zone Code	Soil Type
EQ-X	X	0.05	0.075	0.36	II
EQ-Y	Y	0.05	0.075	0.36	II

Table 11 : Seismic loading as per IS 1893:2002

Load Pattern	I	R	Time Used	Coefficient Used	Weight Used	Base Shear
			Sec		KN	KN
EQ-X	1.	5.	10996.1938	0.17	16141.326	197.57
EQ-Y	1.	5.	0.6814	0.997967	16141.326	1159.812

3.4.4.1 Response spectrum

Response spectrum analysis is done using IS 1893: 2002 design code for earthquake resistant structure. Spectrum is given in table 12-14. Function damping off 0.05 is used for zone 5 and soil type II. Complete quadratic combination (CQC) technique is used for solving response spectrum analysis. Damping of 0.05 is constant throughout the analysis.

Table 12 : Response spectrum

Case	Modal Combo	GMCf1 Cyc/sec	GMCf2 Cyc/sec	Per Rigid	Direction Combo	Motion Type	Damping Type
EQ-X	CQC	1.0000 E+00	0.0000 E+00	SRSS	CQC3	Acceleration	Constant
EQ-Y	CQC	1.0000 E+00	0.0000 E+00	SRSS	CQC3	Acceleration	Constant

Table 13: Response spectrum

Name	Period	Acceleration	Function Damping	Z	Soil Type
	Sec				
spectrum	0.	0.36	0.05	0.36	II
spectrum	0.1	0.9			
spectrum	0.55	0.9			
spectrum	0.8	0.612			
spectrum	1.	0.4896			
spectrum	1.2	0.408			
spectrum	1.4	0.349714			
spectrum	1.6	0.306			
spectrum	1.8	0.272			
spectrum	2.	0.2448			
spectrum	2.5	0.19584			
spectrum	3.	0.1632			
spectrum	3.5	0.139886			
spectrum	4.	0.1224			
spectrum	4.5	0.1224			
spectrum	5.	0.1224			
spectrum	5.5	0.1224			
spectrum	6.	0.1224			
spectrum	6.5	0.1224			
spectrum	7.	0.1224			
spectrum	7.5	0.1224			
spectrum	8.	0.1224			
spectrum	8.5	0.1224			
spectrum	9.	0.1224			
spectrum	9.5	0.1224			
spectrum	10.	0.1224			

Table 14 : Response spectrum

Case	Load Type	Load Name	Coordinate System	Function	Angle	Trans SF
					Degrees	m/sec2
EQ-X	Acceleration	U1	GLOBAL	spectrum	0.	1.
EQ-Y	Acceleration	U2	GLOBAL	spectrum	0.	1.

3.5 Load Case

After defining the load pattern load cases are defined in analysis tab of CSI Bridge. Load cases are defined for analysis of the bridge using initial condition zero. Load cases are given in table 15.

Table 15 : Load case

Case	Type	ML Factor Vertical	Initial Condition	ML Factor Brake	Modal Case	ML Factor Center
DEAD	Lin Static		Zero			
modal	Lin Modal		Zero			
EQ-X	Lin Response Spectrum				modal	
EQ-Y	Lin Response Spectrum				modal	
WEARING	Lin Static		Zero			
FOOTPATH	Lin Static		Zero			
RAILING	Lin Static		Zero			
CLASS-AA WHEELED	Lin Moving	1.	Zero	2.		0.
CLASS-A	Lin Moving	1.	Zero	2.		0.

3.6 Load Combination

In IS1893:2002 different load combinations for bridge design are given. Using those load combination maximum axial force, maximum moment, maximum stress at top and bottom are obtained from the analysis. There are three load cases used in the analysis which are shown in table 16.

Table 16 : Load combination

Combo Name	Combo Type	Case Name	Scale Factor
1.2(DL+LL+EL-X+0.3EL-Y)	Linear Add	DEAD	1.2
1.2(DL+LL+EL-X+0.3EL-Y)		CLASS-A	1.2
1.2(DL+LL+EL-X+0.3EL-Y)		CLASS-AA WHEELED	1.2
1.2(DL+LL+EL-X+0.3EL-Y)		EQ-X	1.2
1.2(DL+LL+EL-X+0.3EL-Y)		EQ-Y	0.36
1.5(DL+EL-X+0.3EL-Y)	Linear Add	DEAD	1.5
1.5(DL+EL-X+0.3EL-Y)		EQ-X	1.5
1.5(DL+EL-X+0.3EL-Y)		EQ-Y	0.45
0.9DL+1.5(EL-X+0.3EL-Y)	Linear Add	DEAD	0.9
0.9DL+1.5(EL-X+0.3EL-Y)		EQ-X	1.5
0.9DL+1.5(EL-X+0.3EL-Y)		EQ-Y	0.45

Chapter 4
ANALYSIS AND RESULT

4.1 Axial force model 1 without stiffness in expansion joint load

Table 17: Axial force model 1

Layout Line Distance m	Item Type	P KN
0	Max	3844.55
0	Min	3121.892
2.3476	Max	3844.55
2.3476	Min	3121.892
2.3476	Max	3844.521
2.3476	Min	3121.92
4.6952	Max	3844.521
4.6952	Min	3121.92
4.6952	Max	3844.472
4.6952	Min	3121.969
7.0428	Max	3844.472
7.0428	Min	3121.969
7.0428	Max	3844.41
7.0428	Min	3122.031
9.3904	Max	3844.41
9.3904	Min	3122.031
9.3904	Max	3844.366
9.3904	Min	3122.075
10	Max	3844.366
10	Min	3122.075
10	Max	-929.082
10	Min	-1278.73
11.738	Max	-929.082
11.738	Min	-1278.73
11.738	Max	-942.278
11.738	Min	-1265.722
14.0856	Max	-942.278
14.0856	Min	-1265.722
14.0856	Max	-957.428
14.0856	Min	-1250.759
16.4332	Max	-957.428
16.4332	Min	-1250.759
16.4332	Max	-972.296
16.4332	Min	-1235.516
18.7808	Max	-972.296
18.7808	Min	-1235.516
18.7808	Max	-984.014
18.7808	Min	-1224.361
20	Max	-984.014
20	Min	-1224.361
20	Max	-191.713
20	Min	-329.349
21.8288	Max	-191.713
21.8288	Min	-329.349
21.8288	Max	-201.396
21.8288	Min	-319.479
23.048	Max	-201.396
23.048	Min	-319.479
23.048	Max	-214.319
23.048	Min	-306.743
25.8288	Max	-214.319
25.8288	Min	-306.743
25.8288	Max	-232.064
25.8288	Min	-288.811
28.6096	Max	-232.064
28.6096	Min	-288.811
28.6096	Max	-245.434
28.6096	Min	-275.441
30	Max	-245.434
30	Min	-275.441
30	Max	205.35
30	Min	168.9
31.3904	Max	205.35
31.3904	Min	168.9
31.3904	Max	218.339
31.3904	Min	155.161
34.1712	Max	218.339
34.1712	Min	155.161
34.1712	Max	236.445
34.1712	Min	137.617
36.952	Max	236.445
36.952	Min	137.617

Layout Line Distance m	Item Type	P KN
36.952	Max	249.547
36.952	Min	125.078
38.1712	Max	249.547
40	Max	125.078
40	Min	259.035
40	Max	115.027
40	Min	259.035
41.2192	Max	115.027
41.2192	Min	745.257
41.2192	Max	498.618
41.2192	Min	745.257
43.5668	Max	498.618
43.5668	Min	756.498
43.5668	Max	487.002
43.5668	Min	756.498
45.9144	Max	487.002
45.9144	Min	771.824
45.9144	Max	472.239
45.9144	Min	771.824
48.262	Max	472.239
48.262	Min	786.682
48.262	Max	457.006
48.262	Min	786.682
50	Max	457.006
50	Min	799.868
50	Max	444.007
50	Min	799.868
50.6096	Max	444.007
50.6096	Min	17740.616
50.6096	Max	17018.919
50.6096	Min	17740.616
52.9572	Max	17018.919
52.9572	Min	17740.66
52.9572	Max	17018.875
52.9572	Min	17740.66
55.3048	Max	17018.875
55.3048	Min	17740.723
55.3048	Max	17018.812
55.3048	Min	17740.723
57.6524	Max	17018.812
60	Max	17740.773
60	Min	17018.763

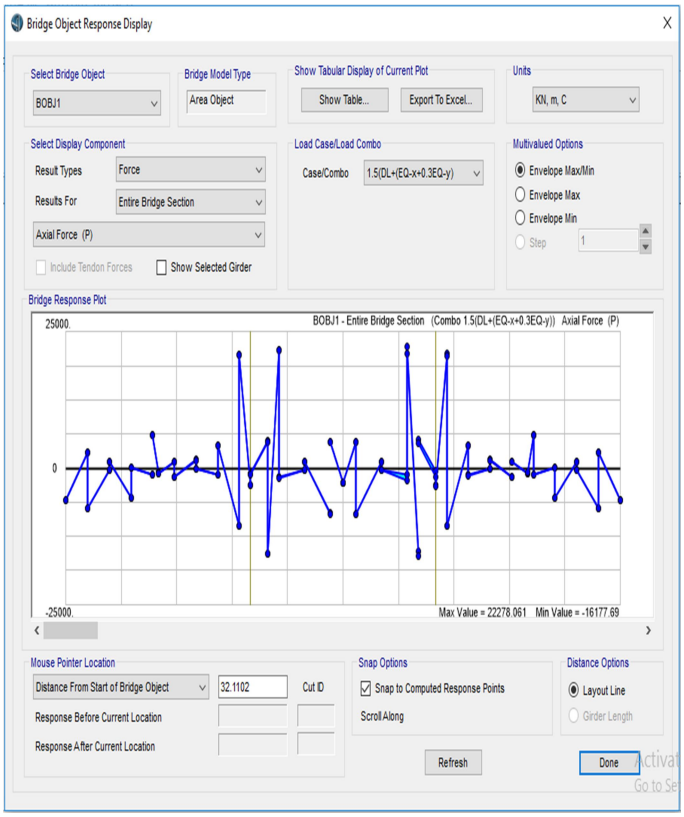

Figure 8 axial force model 1

4.2 Axial force model 2 lead rubber bearing

Table 18: Axial force model 2

Layout Line Distance m	Item Type	P KN
0	Max	-7671.214
0	Min	-7971.259
2.3476	Max	3935.532
2.3476	Min	3393.35
2.3476	Max	-10403.037
2.3476	Min	-10644.576
4.6952	Max	398.754
4.6952	Min	-69.513
4.6952	Max	-106.083
4.6952	Min	-522.89
7.0428	Max	-1855.896
7.0428	Min	-2376.2
7.0428	Max	-93.363
7.0428	Min	-527.365
9.3904	Max	-437.958
9.3904	Min	-896.075
9.3904	Max	322.388
9.3904	Min	-91.503
10	Max	-244.771
10	Min	-687.655
10	Max	-175.62
10	Min	-619.949
11.738	Max	-344.305
11.738	Min	-695.734
11.738	Max	54.69
11.738	Min	-449.998
14.0856	Max	-1332.978
14.0856	Min	-1603.217
14.0856	Max	-32.13
14.0856	Min	-450.82
16.4332	Max	-902.814
16.4332	Min	-1260.225
16.4332	Max	1980.649
16.4332	Min	1503.589
18.7808	Max	-4603.492
18.7808	Min	-5017.241
18.7808	Max	8324.913
18.7808	Min	8082.481
20	Max	-1465.531
20	Min	-1874.767
20	Max	-806.565
20	Min	-822.922
21.8288	Max	1925.94
21.8288	Min	1803.298
21.8288	Max	-7354.639
21.8288	Min	-7407.212
23.048	Max	8961.381
23.048	Min	8931.422
23.048	Max	-1087.996
23.048	Min	-1162.287
25.8288	Max	-434.821
25.8288	Min	-456.607
25.8288	Max	-468.376
25.8288	Min	-560.952
28.6096	Max	-863.368
28.6096	Min	-901.664
28.6096	Max	-348.26
28.6096	Min	-378.655
30	Max	-386.074
30	Min	-390.034
30	Max	-454.138
30	Min	-458.091
31.3904	Max	-66.342
31.3904	Min	-96.731
31.3904	Max	-1266.996
31.3904	Min	-1305.301
34.1712	Max	639.194
34.1712	Min	546.623
34.1712	Max	-761.355
34.1712	Min	-783.133
36.952	Max	1028.041
36.952	Min	953.748

Layout Line Distance m	Item Type	P KN
36.952	Max	-938.545
36.952	Min	-968.504
38.1712	Max	1577.988
40	Max	1525.414
40	Min	666.599
40	Max	543.955
40	Min	872.865
41.2192	Max	856.507
41.2192	Min	1302.009
41.2192	Max	892.77
41.2192	Min	-1230.7
43.5668	Max	-1473.137
43.5668	Min	1926.146
43.5668	Max	1512.396
43.5668	Min	899.511
45.9144	Max	422.447
45.9144	Min	1021.06
45.9144	Max	663.646
45.9144	Min	914.232
48.262	Max	495.539
48.262	Min	1049.842
48.262	Max	779.601
48.262	Min	982.009
50	Max	477.318
50	Min	917.109
50	Max	565.678
50	Min	964.003
50.6096	Max	519.671
50.6096	Min	949.713
50.6096	Max	506.826
50.6096	Min	991.981
52.9572	Max	578.087
52.9572	Min	952.594
52.9572	Max	494.474
52.9572	Min	958.696
55.3048	Max	524.691
55.3048	Min	-1282.375
55.3048	Max	-1523.914
55.3048	Min	1897.554
57.6524	Max	1355.367
60	Max	-739.27
60	Min	-1039.317

Figure 9 axial force model 2

4.3 Axial force model 3 rubber isolator in expansion joint

Table 19: Axial force model 3

Layout Line Distance m	Item Type	P KN
0	Max	-367.991
0	Min	-637.963
2.3476	Max	769.139
2.3476	Min	283.215
2.3476	Max	-542.487
2.3476	Min	-760.973
4.6952	Max	420.592
4.6952	Min	0.837
4.6952	Max	389.867
4.6952	Min	16.252
7.0428	Max	298.972
7.0428	Min	-167.665
7.0428	Max	385.158
7.0428	Min	-3.886
9.3904	Max	382.484
9.3904	Min	-28.223
9.3904	Max	402.793
9.3904	Min	31.816
10	Max	379.805
10	Min	-17.23
10	Max	384.404
10	Min	-13.914
11.738	Max	353.152
11.738	Min	38.107
11.738	Max	383.078
11.738	Min	-69.323
14.0856	Max	342.692
14.0856	Min	100.417
14.0856	Max	374.772
14.0856	Min	-0.538
16.4332	Max	402.495
16.4332	Min	82.103
16.4332	Max	436.991
16.4332	Min	9.414
18.7808	Max	1006.535
18.7808	Min	635.494
18.7808	Max	-1074.71
18.7808	Min	-1292.35
20	Max	598.715
20	Min	231.899
20	Max	263.654
20	Min	248.577
21.8288	Max	57.513
21.8288	Min	-52.435
21.8288	Max	817.091
21.8288	Min	767.094
23.048	Max	-590.972
23.048	Min	-623.289
23.048	Max	259.303
23.048	Min	192.589
25.8288	Max	210.82
25.8288	Min	191.269
25.8288	Max	257.81
25.8288	Min	174.744
28.6096	Max	200.349
28.6096	Min	165.996
28.6096	Max	238.751
28.6096	Min	211.481
30	Max	148.65
30	Min	145.1
30	Max	204.565
30	Min	201.018
31.3904	Max	-56.028
31.3904	Min	-83.295
31.3904	Max	977.847
31.3904	Min	943.491
34.1712	Max	-966.113
34.1712	Min	-1049.18
34.1712	Max	631.985
34.1712	Min	612.437
36.952	Max	-914.299
36.952	Min	-981.014

Layout Line Distance m	Item Type	P KN
36.952	Max	-1078.36
36.952	Min	-1445.18
38.1712	Max	5428.201
40	Max	5210.554
40	Min	-3149.91
40	Max	-3520.95
40	Min	1363.757
41.2192	Max	936.178
41.2192	Min	-675.917
41.2192	Max	-996.311
41.2192	Min	-68.536
43.5668	Max	-443.847
43.5668	Min	-1020.74
43.5668	Max	-1263.01
43.5668	Min	-34.892
45.9144	Max	-487.294
45.9144	Min	-308.345
45.9144	Max	-623.392
45.9144	Min	-183.408
48.262	Max	-581.727
48.262	Min	-225.862
48.262	Max	-622.898
48.262	Min	120.872
50	Max	-250.107
50	Min	-342.775
50	Max	-753.483
50	Min	-133.11
50.6096	Max	-522.155
50.6096	Min	-1215.65
50.6096	Max	-1682.29
50.6096	Min	-129.048
52.9572	Max	-502.664
52.9572	Min	143.536
52.9572	Max	-276.221
52.9572	Min	-6281.57
55.3048	Max	-6500.05
55.3048	Min	2262.447
55.3048	Max	1776.521
55.3048	Min	-4688.34
57.6524	Max	-4958.31
60	Max	2262.447
60	Min	1776.521

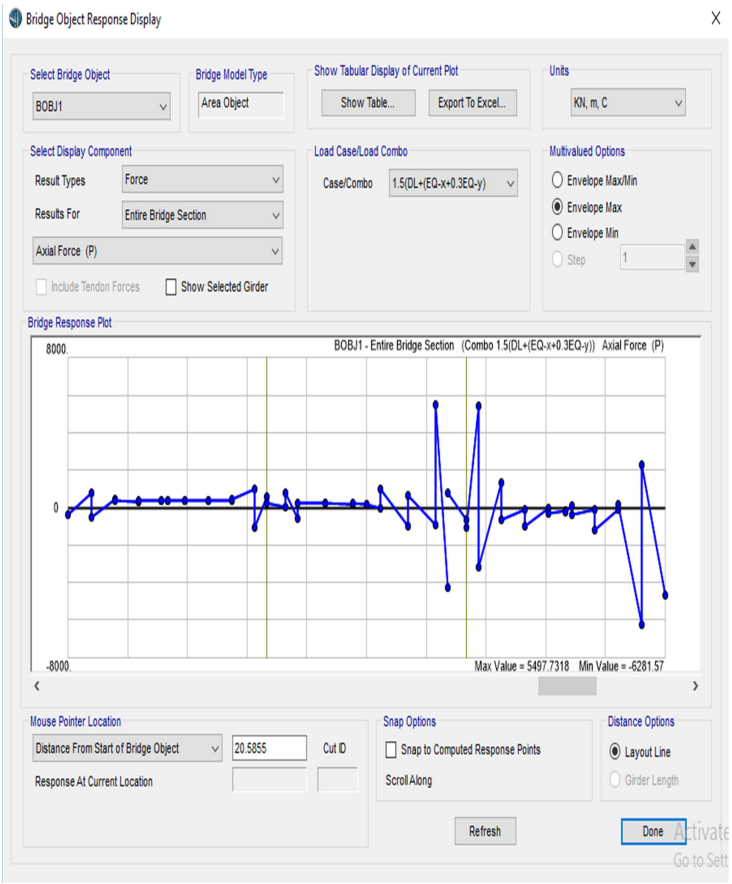

Figure 10 axial force model 3

. 4.4 Axial force model 4 HDRB

Table 20: Axial force model 4

Layout Line Distance m	Item Type	P KN
0	Max	684.089
0	Min	-684.089
2.3476	Max	-951.631
2.3476	Min	963.085
2.3476	Max	509.458
2.3476	Min	-983.299
4.6952	Max	-1206.83
4.6952	Min	459.119
4.6952	Max	62.809
4.6952	Min	401.505
7.0428	Max	47.842
7.0428	Min	243.329
7.0428	Max	-200.572
7.0428	Min	399.185
9.3904	Max	31.037
9.3904	Min	382.829
9.3904	Max	-6.266
9.3904	Min	433.381
10	Max	82.887
10	Min	387.925
10	Max	12.049
10	Min	395.517
11.738	Max	20.14
11.738	Min	356.391
11.738	Max	74.701
11.738	Min	404.794
14.0856	Max	-24.751
14.0856	Min	345.496
14.0856	Max	154.69
14.0856	Min	373.043
16.4332	Max	27.707
16.4332	Min	375.252
16.4332	Max	97.212
16.4332	Min	430.685
18.7808	Max	20.114
18.7808	Min	692.233
18.7808	Max	-418.902
18.7808	Min	-633.74
20	Max	477.872
20	Min	182.132
20	Max	265.035
20	Min	194.823
21.8288	Max	141.755
21.8288	Min	30.788
21.8288	Max	600.556
21.8288	Min	500.451
23.048	Max	-123.739
23.048	Min	-150.768
23.048	Max	253.858
23.048	Min	166.068
25.8288	Max	233.238
25.8288	Min	205.386
25.8288	Max	216.869
25.8288	Min	111.779
28.6096	Max	264.659
28.6096	Min	221.65
28.6096	Max	210.231
28.6096	Min	175.114
30	Max	179.911
30	Min	174.999
30	Max	213.577
30	Min	208.667
31.3904	Max	-8.879
31.3904	Min	-43.994
31.3904	Max	1031.635
31.3904	Min	988.624
34.1712	Max	-711.272
34.1712	Min	-816.36
34.1712	Max	593.859
34.1712	Min	566.01
36.952	Max	-604.635
36.952	Min	-692.426

Layout Line Distance m	Item Type	P KN
36.952	Max	1296.311
36.952	Min	1269.282
38.1712	Max	-1262
40	Max	-1362.1
40	Min	-188.586
40	Max	-299.553
40	Min	-470.483
41.2192	Max	-540.695
41.2192	Min	-556.295
41.2192	Max	-852.035
41.2192	Min	1474.489
43.5668	Max	1259.649
43.5668	Min	-1205.86
43.5668	Max	-1501.37
43.5668	Min	339.76
45.9144	Max	-70.812
45.9144	Min	-424.89
45.9144	Max	-702.931
45.9144	Min	-193.738
48.262	Max	-539.075
48.262	Min	-575.777
48.262	Max	-766.584
48.262	Min	-191.822
50	Max	-621.368
50	Min	-288.943
50	Max	-570.633
50	Min	-233.013
50.6096	Max	-608.39
50.6096	Min	-246.949
50.6096	Max	-622.827
50.6096	Min	-88.56
52.9572	Max	-439.055
52.9572	Min	-299.679
52.9572	Max	-688.775
52.9572	Min	-204.437
55.3048	Max	-572.587
55.3048	Min	-2797.67
55.3048	Max	-3021.2
55.3048	Min	794.985
57.6524	Max	341.357
60	Max	-2177.61
60	Min	-2445.16

Figure 11 axial force model 4

4.5 Moment model 1 without stiffness in expansion joint

Table 21: Moment model 1

Layout Line Distance m	Item Type	M3 KNm
0	Max	-21732.2
0	Min	-23051.3
2.3476	Max	-14069.1
2.3476	Min	-15141.3
2.3476	Max	-14069.1
2.3476	Min	-15141.2
4.6952	Max	-7538.16
4.6952	Min	-8366.59
4.6952	Max	-7538.23
4.6952	Min	-8366.52
7.0428	Max	-2137.67
7.0428	Min	-2729.03
7.0428	Max	-2137.73
7.0428	Min	-2728.97
9.3904	Max	2136.295
9.3904	Min	1767.511
9.3904	Max	2136.303
9.3904	Min	1767.503
10	Max	3063.161
10	Min	2747.223
10	Max	1511.752
10	Min	1049.623
11.738	Max	1066.984
11.738	Min	669.016
11.738	Max	1055.398
11.738	Min	680.3105
14.0856	Max	-527.477
14.0856	Min	-824.002
14.0856	Max	-539.893
14.0856	Min	-811.234
16.4332	Max	-3247.32
16.4332	Min	-3458.61
16.4332	Max	-3257.7
16.4332	Min	-3448.57
18.7808	Max	-7079.67
18.7808	Min	-7249.6

Layout Line Distance m	Item Type	M3 KNm
18.7808	Max	-7082.48
18.7808	Min	-7247.05
20	Max	-9503.8
20	Min	-9678.61
20	Max	-10973.5
20	Min	-11376.6
21.8288	Max	-7204.21
21.8288	Min	-7551.83
21.8288	Max	-7211.67
21.8288	Min	-7544.21
23.048	Max	-5080.67
23.048	Min	-5374.33
23.048	Max	-5090.22
23.048	Min	-5364.48
25.8288	Max	-1379.08
25.8288	Min	-1558.55
25.8288	Max	-1392.4
25.8288	Min	-1545.77
28.6096	Max	725.4668
28.6096	Min	673.9876
28.6096	Max	716.3725
28.6096	Min	681.6826
30	Max	1197.425
30	Min	1175.63
30	Max	109.5055
30	Min	93.9167
31.3904	Max	4382.414
31.3904	Min	4344.008
31.3904	Max	4392.282
31.3904	Min	4335.635
34.1712	Max	11771.59
34.1712	Min	11613.58
34.1712	Max	11785
34.1712	Min	11600.61
36.952	Max	17570.65
36.952	Min	17291.84

Layout Line Distance m	Item Type	M3 KNm
36.952	Max	17579.98
36.952	Min	17281.68
38.1712	Max	19613.47
40	Max	19276.44
40	Min	19621.49
40	Max	19269.34
40	Min	22097.32
41.2192	Max	21689.88
41.2192	Min	28484.34
41.2192	Max	28309.52
41.2192	Min	25855.49
43.5668	Max	25689.49
43.5668	Min	25858.89
43.5668	Max	25686.98
43.5668	Min	19955.15
45.9144	Max	19760.05
45.9144	Min	19965.7
45.9144	Max	19749.94
45.9144	Min	12947.2
48.262	Max	12670.5
48.262	Min	12959.97
48.262	Max	12658.06
48.262	Min	4816.723
50	Max	4435.93
50	Min	4827.833
50	Max	4424.174
50	Min	-1928.27
50.6096	Max	-2396.23
50.6096	Min	7558.356
50.6096	Max	7242.634
50.6096	Min	2443.197
52.9572	Max	2074.698
52.9572	Min	2443.189
52.9572	Max	2074.706
52.9572	Min	-17960.1
55.3048	Max	-18550.9
55.3048	Min	-62150
55.3048	Max	-63221.4
55.3048	Min	-62149.9
57.6524	Max	-63221.5
60	Max	-85942.2
60	Min	-87260.7

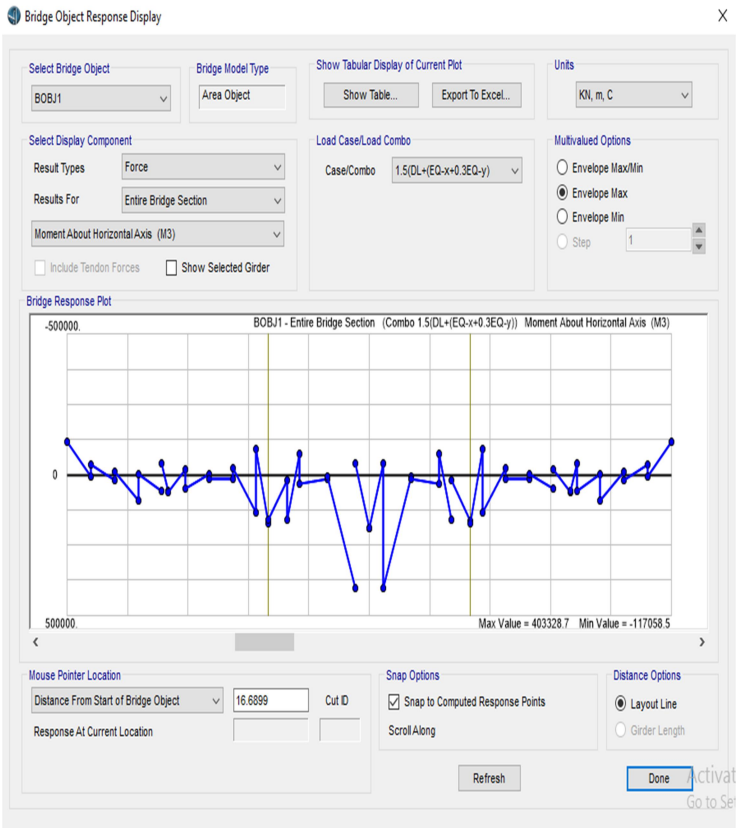

Figure 12 moment model 1

4.6 Moment model 2 lead rubber bearing in expansion joint

Table 22: Moment model 2

Layout Line Distance m	Item Type	M3 KNm
0	Max	-146816
0	Min	-149171
2.3476	Max	5408.078
2.3476	Min	5378.299
2.3476	Max	-42512.5
2.3476	Min	-42738.7
4.6952	Max	3634.734
4.6952	Min	3465.466
4.6952	Max	-9784.77
4.6952	Min	-9833.77
7.0428	Max	8772.527
7.0428	Min	8027.326
7.0428	Max	-3131.76
7.0428	Min	-3165.91
9.3904	Max	1229.221
9.3904	Min	712.4729
9.3904	Max	-2907.29
9.3904	Min	-3231.67
10	Max	1099.924
10	Min	560.286
10	Max	626.878
10	Min	45.3439
11.738	Max	2231.58
11.738	Min	2019.315
11.738	Max	187.979
11.738	Min	-277.194
14.0856	Max	8672.872
14.0856	Min	8477.454
14.0856	Max	458.6456
14.0856	Min	335.7269
16.4332	Max	6991.961
16.4332	Min	6967.331
16.4332	Max	-15279.1
16.4332	Min	-15436.2
18.7808	Max	56040.68
18.7808	Min	55785.74

Layout Line Distance m	Item Type	M3 KNm
18.7808	Max	-39092
18.7808	Min	-39401.7
20	Max	70131.24
20	Min	69622.35
20	Max	66524.24
20	Min	65339.7
21.8288	Max	6836.103
21.8288	Min	6808.447
21.8288	Max	65995.71
21.8288	Min	65604.34
23.048	Max	-34606.9
23.048	Min	-34785.3
23.048	Max	12038.28
23.048	Min	11957.86
25.8288	Max	1285.505
25.8288	Min	1273.122
25.8288	Max	4476.647
25.8288	Min	4437.206
28.6096	Max	-1650.89
28.6096	Min	-1682.13
28.6096	Max	1707.486
28.6096	Min	1689.224
30	Max	262.7975
30	Min	259.2499
30	Max	773.7762
30	Min	770.2199
31.3904	Max	-1554.96
31.3904	Min	-1573.23
31.3904	Max	3996.612
31.3904	Min	3965.363
34.1712	Max	-3398.97
34.1712	Min	-3438.41
34.1712	Max	-1001.65
34.1712	Min	-1014.03
36.952	Max	-4356.53
36.952	Min	-4436.95

Layout Line Distance m	Item Type	M3 KNm
36.952	Max	10308.37
36.952	Min	10129.9
38.1712	Max	-15063.6
40	Max	-15454.9
40	Min	-3464.05
40	Max	-3491.71
40	Min	-16060.4
41.2192	Max	-17245
41.2192	Min	-17558.6
41.2192	Max	-18067.5
41.2192	Min	10583.91
43.5668	Max	10274.14
43.5668	Min	-13951.8
43.5668	Max	-14206.7
43.5668	Min	4412.885
45.9144	Max	4255.76
45.9144	Min	-1358.33
45.9144	Max	-1382.96
45.9144	Min	79.7587
48.262	Max	-43.161
48.262	Min	-1129.85
48.262	Max	-1325.27
48.262	Min	-328.756
50	Max	-793.932
50	Min	246.7918
50	Max	34.5246
50	Min	-627.221
50.6096	Max	-1208.76
50.6096	Min	-551.293
50.6096	Max	-1090.94
50.6096	Min	271.2218
52.9572	Max	-53.1553
52.9572	Min	-466.851
52.9572	Max	-983.603
52.9572	Min	-504.392
55.3048	Max	-538.542
55.3048	Min	-7974.62
55.3048	Max	-8200.77
55.3048	Min	1089.297
57.6524	Max	1059.519
60	Max	-30313.6
60	Min	-32668.8

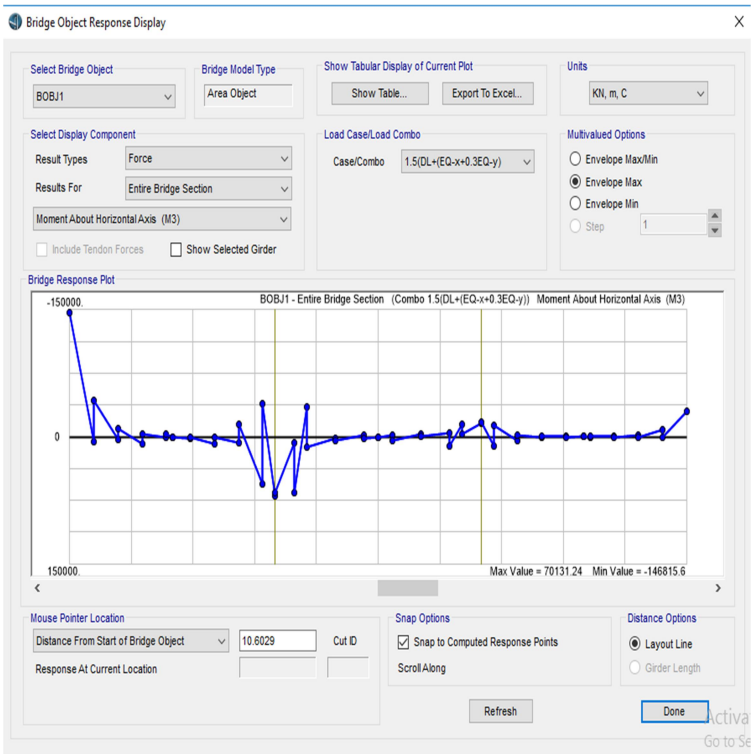

Figure 13 moment model 2

4.7 Moment model 3 rubber isolator in expansion joint load

Table 23: Moment model 3

Layout Line Distance m	Item Type	M3 KNm
0	Max	-12511.4278
0	Min	-14648.1289
2.3476	Max	586.5128
2.3476	Min	556.5126
2.3476	Max	-3498.7346
2.3476	Min	-3726.3132
4.6952	Max	447.9135
4.6952	Min	295.71
4.6952	Max	-685.2122
4.6952	Min	-735.2418
7.0428	Max	709.3635
7.0428	Min	40.7604
7.0428	Max	-137.2037
7.0428	Min	-168.727
9.3904	Max	108.2676
9.3904	Min	-354.9949
9.3904	Max	131.9369
9.3904	Min	-158.9838
10	Max	63.8375
10	Min	-419.9363
10	Max	106.0687
10	Min	-415.2577
11.738	Max	-225.9487
11.738	Min	-416.3054
11.738	Max	191.9799
11.738	Min	-225.0492
14.0856	Max	-1375.9747
14.0856	Min	-1551.8449
14.0856	Max	-14.6992
14.0856	Min	-124.8775
16.4332	Max	-1273.3627
16.4332	Min	-1299.599
16.4332	Max	2764.5946
16.4332	Min	2621.0013
18.7808	Max	-9567.7701
18.7808	Min	-9822.019

Layout Line Distance m	Item Type	M3 KNm
18.7808	Max	6955.5036
18.7808	Min	6667.5595
20	Max	-11619.5685
20	Min	-12096.0135
20	Max	-10502.7362
20	Min	-11573.4103
21.8288	Max	-2641.7485
21.8288	Min	-2669.5839
21.8288	Max	-10215.9957
21.8288	Min	-10591.9016
23.048	Max	3165.5747
23.048	Min	2990.1553
23.048	Max	-4092.1018
23.048	Min	-4167.8613
25.8288	Max	-1535.4145
25.8288	Min	-1546.6452
25.8288	Max	-3158.6549
25.8288	Min	-3194.9981
28.6096	Max	2108.108
28.6096	Min	2079.6303
28.6096	Max	-1660.8552
28.6096	Min	-1677.5182
30	Max	110.9304
30	Min	107.7129
30	Max	-286.3977
30	Min	-289.6189
31.3904	Max	855.7213
31.3904	Min	839.0575
31.3904	Max	-1964.721
31.3904	Min	-1993.2069
34.1712	Max	2390.3055
34.1712	Min	2353.9618
34.1712	Max	270.3274
34.1712	Min	259.097
36.952	Max	7047.8809
36.952	Min	6972.123

Layout Line Distance m	Item Type	M3 KNm
36.952	Max	-25122.1315
36.952	Min	-25297.554
38.1712	Max	42323.6898
40	Max	41947.7887
40	Min	4342.9435
40	Max	4315.1075
40	Min	43249.0022
41.2192	Max	42178.3324
41.2192	Min	45485.8051
41.2192	Max	45009.3525
41.2192	Min	-25477.7957
43.5668	Max	-25765.7442
43.5668	Min	36092.4188
43.5668	Max	35838.1659
43.5668	Min	-10138.7956
45.9144	Max	-10282.391
45.9144	Min	4187.5241
45.9144	Max	4161.288
45.9144	Min	193.4693
48.262	Max	83.2906
48.262	Min	5087.7544
48.262	Max	4911.8827
48.262	Min	366.2193
50	Max	-50.8114
50	Min	1156.0996
50	Max	965.7419
50	Min	691.0481
50.6096	Max	169.7197
50.6096	Min	927.3174
50.6096	Max	443.5418
50.6096	Min	-1786.8073
52.9572	Max	-2077.7289
52.9572	Min	1008.6137
52.9572	Max	545.3496
52.9572	Min	-1829.2354
55.3048	Max	-1860.7591
55.3048	Min	-25601.6523
55.3048	Max	-25829.2338
55.3048	Min	3335.6728
57.6524	Max	3305.6728
60	Max	-87703.4187
60	Min	-89840.1413

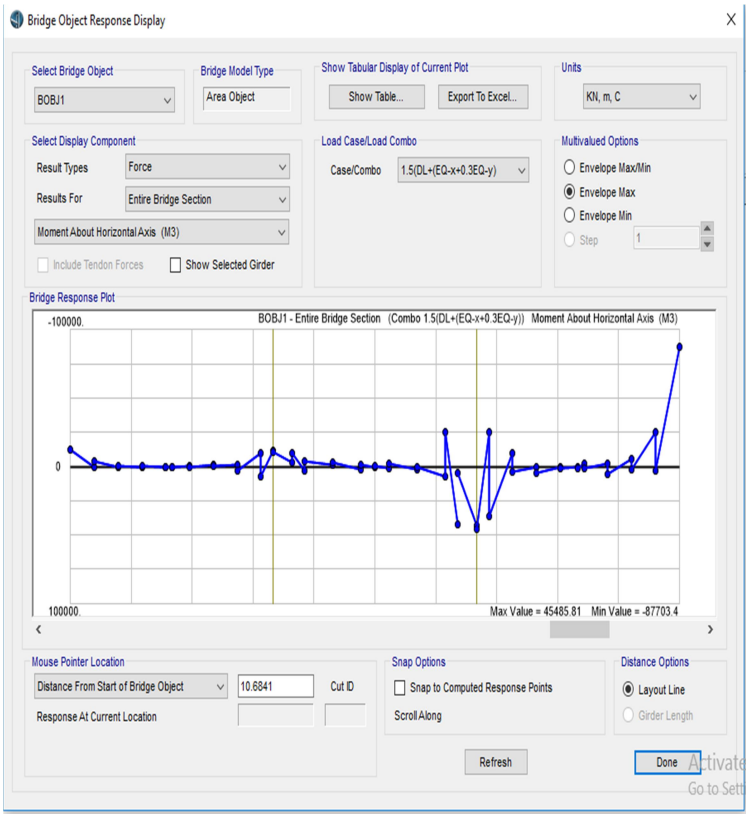

Figure 14 moment model

4.8 Moment model 4 high damping rubber isolator in expansion joint load

Table 24: Moment model 4

Layout Line Distance m	Item Type	M3 KNm
0	Max	-19310.5545
0	Min	-21147.9154
2.3476	Max	816.384
2.3476	Min	780.4448
2.3476	Max	-5379.5575
2.3476	Min	-5590.2226
4.6952	Max	577.5259
4.6952	Min	428.5107
4.6952	Max	-1123.7608
4.6952	Min	-1171.0079
7.0428	Max	999.4223
7.0428	Min	354.0415
7.0428	Max	-287.7969
7.0428	Min	-313.6746
9.3904	Max	90.8437
9.3904	Min	-348.3497
9.3904	Max	15.2111
9.3904	Min	-264.9869
10	Max	39.0545
10	Min	-419.3521
10	Max	50.2092
10	Min	-443.0532
11.738	Max	-97.5421
11.738	Min	-274.4655
11.738	Max	138.7107
11.738	Min	-256.1446
14.0856	Max	-823.9368
14.0856	Min	-982.1281
14.0856	Max	-26.9604
14.0856	Min	-132.9009
16.4332	Max	-812.0049
16.4332	Min	-837.2295
16.4332	Max	1420.6142
16.4332	Min	1299.6705
18.7808	Max	-5221.2093
18.7808	Min	-5396.7129

Layout Line Distance m	Item Type	M3 KNm
18.7808	Max	3690.5169
18.7808	Min	3515.509
20	Max	-6285.0725
20	Min	-6565.1527
20	Max	-5631.1942
20	Min	-6382.2968
21.8288	Max	-1327.7006
21.8288	Min	-1347.3725
21.8288	Max	-5713.0815
21.8288	Min	-6035.9472
23.048	Max	1809.6244
23.048	Min	1651.8784
23.048	Max	-2278.0439
23.048	Min	-2340.964
25.8288	Max	-933.6686
25.8288	Min	-941.4488
25.8288	Max	-1622.9706
25.8288	Min	-1652.0655
28.6096	Max	886.4006
28.6096	Min	863.3483
28.6096	Max	-897.5167
28.6096	Min	-910.5401
30	Max	-34.944
30	Min	-37.7529
30	Max	-183.3696
30	Min	-186.1815
31.3904	Max	74.4674
31.3904	Min	61.4434
31.3904	Max	-714.8123
31.3904	Min	-737.871
34.1712	Max	438.2511
34.1712	Min	409.1558
34.1712	Max	-223.3736
34.1712	Min	-231.1536
36.952	Max	1645.1442
36.952	Min	1582.2252

Layout Line Distance m	Item Type	M3 KNm
36.952	Max	-9429.9205
36.952	Min	-9587.6692
38.1712	Max	12688.3118
40	Max	12365.4493
40	Min	1211.9768
40	Max	1192.3048
40	Min	13331.2671
41.2192	Max	12580.1677
41.2192	Min	13857.0994
41.2192	Max	13577.0154
41.2192	Min	-7808.4405
43.5668	Max	-7983.4509
43.5668	Min	10850.0685
43.5668	Max	10674.5639
43.5668	Min	-3141.6246
45.9144	Max	-3262.5697
45.9144	Min	1035.1843
45.9144	Max	1009.96
45.9144	Min	82.601
48.262	Max	-23.3398
48.262	Min	1086.7751
48.262	Max	928.5827
48.262	Min	643.2949
50	Max	248.4383
50	Min	66.1236
50	Max	-110.8006
50	Min	832.9986
50.6096	Max	339.7346
50.6096	Min	849.4749
50.6096	Max	391.0668
50.6096	Min	-874.2775
52.9572	Max	-1154.4762
52.9572	Min	887.6833
52.9572	Max	448.4886
52.9572	Min	-732.9113
55.3048	Max	-758.7891
55.3048	Min	-11252.4781
55.3048	Max	-11463.1442
55.3048	Min	1579.176
57.6524	Max	1543.237
60	Max	-37381.3048
60	Min	-39218.6799

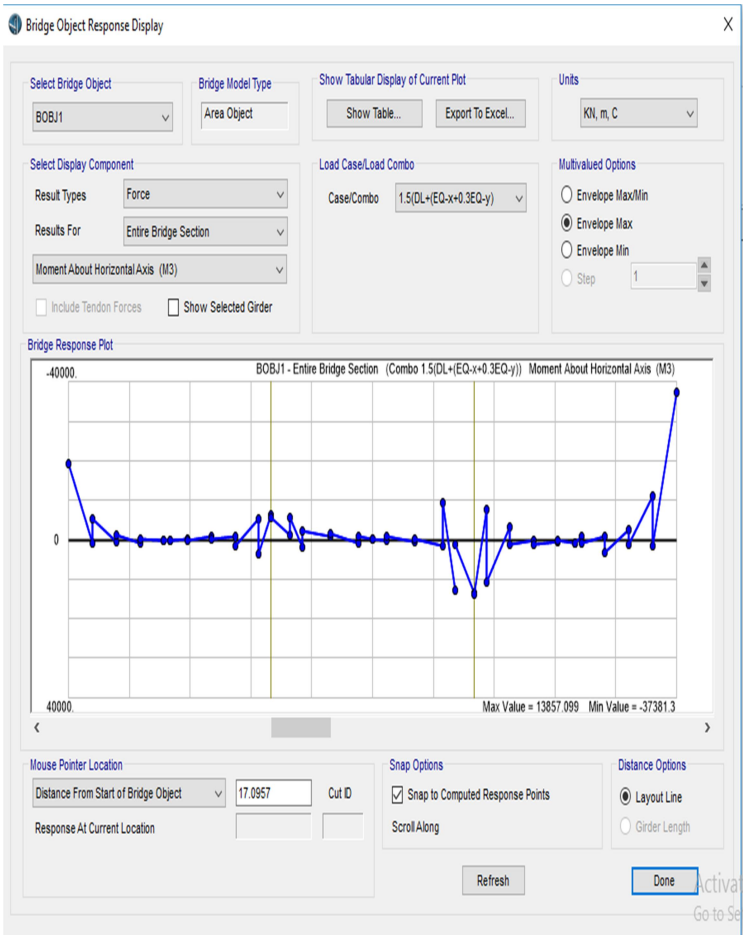

Figure 15 moment model 4

Chapter 5
COMPARISON OF RESULTS

5.1 General

Four different models are analysed to overcome the pounding force generated on the bridge. Lead rubber bearing, rubber isolator and high damping rubber bearing were used in the expansion joint. So to obtain the best suited model of bridge comparison of all the results obtained from analysis of model 1, model 2, model 3 and model 4 are compared in this chapter. In this chapter maximum axial force, maximum moment, maximum stress at top and bottom of bridge and maximum displacement of four bridge models are compared. Three load cases give the most critical values of analysis result. All the load case result obtains from analysis are compared for all models.

5.2 Maximum Axial Force of models

In this section of thesis maximum axial force is calculated from analysis of all four models. Axial force represents the pounding force in the bridge. High axial force can result in collision of bridge deck and could result in damage to bridge. So all the critical or maximum forces were compared to obtain best suited model.

5.2.1 Maximum axial force of model 1

In model 1 we have provided expansion joints which have no stiffness to overcome the pounding force so it will give maximum value of pounding force in comparison to other three models. After analysing model 1 without stiffness in expansion joint all the axial force for three different load combinations are obtained. For load case 1 axial force is 22278.061 KN, for load case 2 axial force is 19065.34 KN and for load case 3 axial force obtain is 13548.433 KN. Maximum axial force for model 1 is given in table 25

Table 25: Maximum axial force model 1

LOAD COMBINATION	AXIAL FORCE (KN)
1.5(DL+(EQx+0.3EQy)	22278.061
1.2(DL+LL+(EQx+0.3EQy)	19065.34
0.9(DL+1.5(EQx+0.3EQy)	13548.433

As shown in figure 16 pounding force is shown in y axis and load cases are in x axis. Maximum axial force for load case1 is much higher than load case 2 and 3. So load case 1 is most critical for model 1 (without stiffness in expansion joint).

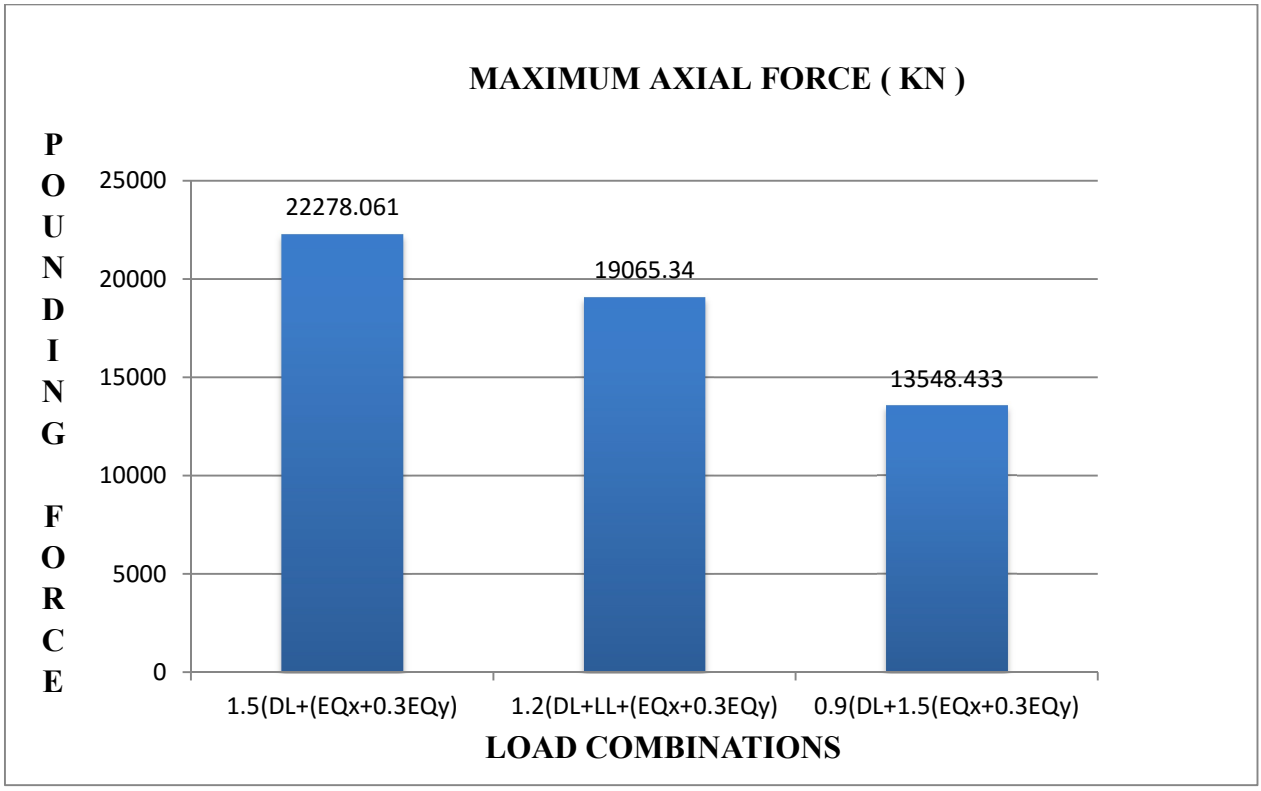

Figure 16: Maximum Axial force model 1

5.2.2 Maximum axial force model 2

In this model 2 lead rubber bearing is being provided to overcome the pounding force. After analysing the model 2 lead rubber bearing for all three load cases we obtain that load case 1 has maximum axial force of 8961.3811 KN and load case 2 has maximum axial force of 7801.28 KN. Similarly for load case 3 has maximum axial force of 5381.3226 KN. Maximum axial force for model 2 is given in table 26

Table 26: Maximum axial force model 2

LOAD COMBINATION	AXIAL FORCE (KN)
1.5(DL+(EQx+0.3EQy)	8961.3811
1.2(DL+LL+(EQx+0.3EQy)	7801.28
0.9(DL+1.5(EQx+0.3EQy)	5381.3226

Figure 17 shows maximum axial force for model 2. As shown in figure 17 pounding force is shown in y axis and load cases are in x axis. Maximum axial force for load case1 is much higher than load case 2 and 3. So load case 1 is most critical for model 1 (lead rubber bearing in expansion joint).

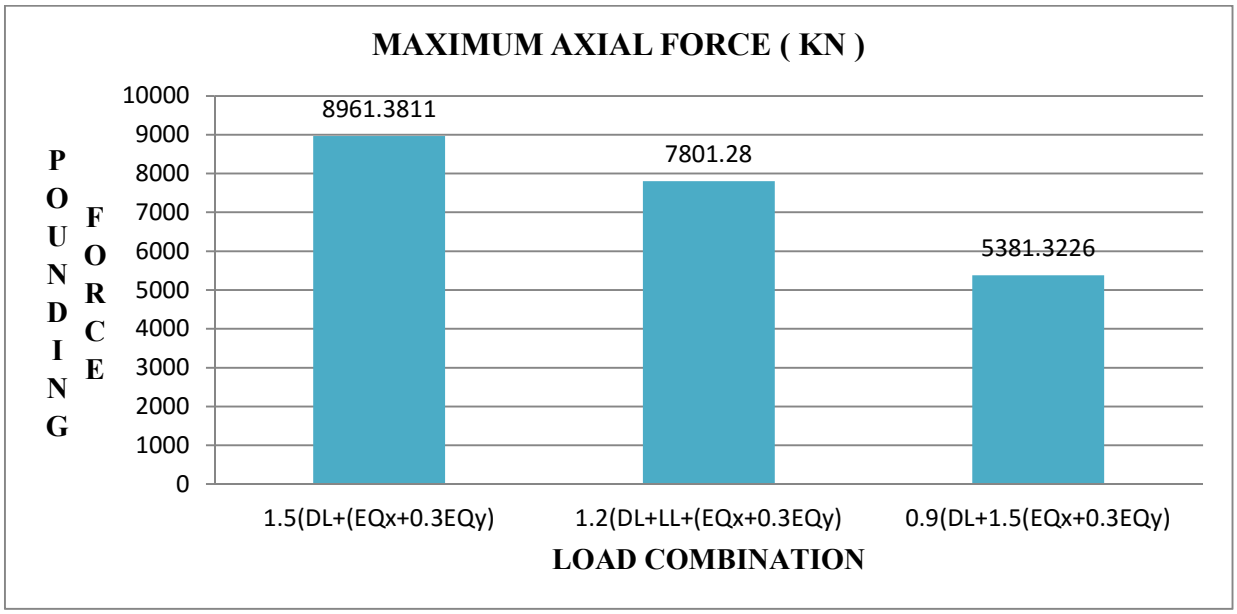

Figure 17: Maximum Axial force model 2

5.2.3 Maximum axial force model 3

In this model rubber isolator bearing is being provided to overcome the pounding force. After analysing the model 3 lead rubber bearing for all three load cases we obtain that load case 1 has maximum axial force of 5497.7318 KN and load case 2 has maximum axial force of 4864.741 KN. Similarly for load case 3 has maximum axial force of 3303.4867 KN. Maximum axial force for model 3 is given in table 27

Table 27: Maximum axial force model 3

LOAD COMBINATION	AXIAL FORCE (KN)
1.5(DL+(EQx+0.3EQy)	5497.7318
1.2(DL+LL+(EQx+0.3EQy)	4864.741
0.9(DL+1.5(EQx+0.3EQy)	3303.4867

Figure 18 shows maximum axial force for model 3. As shown in figure 18 pounding force is shown in y axis and load cases are in x axis. Maximum axial force for load case1 is much higher than load case 2 and 3. So load case 1 is most critical for model 1 (rubber isolator bearing in expansion joint).

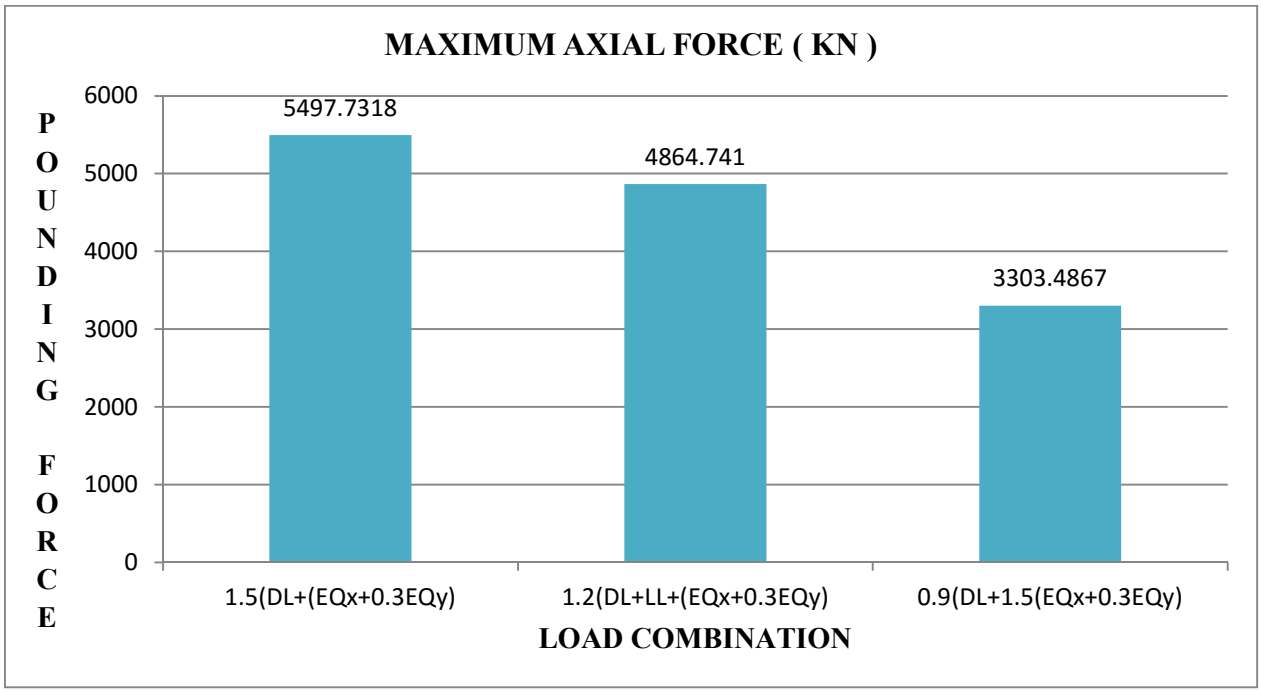

Figure 18: Maximum Axial force model 3

5.2.4 Maximum axial force model 4

In this model lead rubber bearing is being provided to overcome the pounding force. After analysing the model 4 high damping rubber bearing for all three load cases we obtain that load case 1 has maximum axial force of 8961.3811 KN and load case 2 has maximum axial force of 7801.28 KN. Similarly for load case 3 has maximum axial force of 5381.3226 KN. Maximum axial force for model 4 is given in table 28

Table 28: Maximum axial force model 4

LOAD COMBINATION	AXIAL FORCE (KN)
1.5(DL+(EQx+0.3EQy)	1474.4891
1.2(DL+LL+(EQx+0.3EQy)	1541.2825
0.9(DL+1.5(EQx+0.3EQy)	916.9195

Figure 19 shows maximum axial force for model 4. As shown in figure 19 pounding force is shown in y axis and load cases are in x axis. Maximum axial force for load case1 is much higher than load case 2 and 3. So load case 1 is most critical for model 1 (high damping rubber bearing in expansion joint).

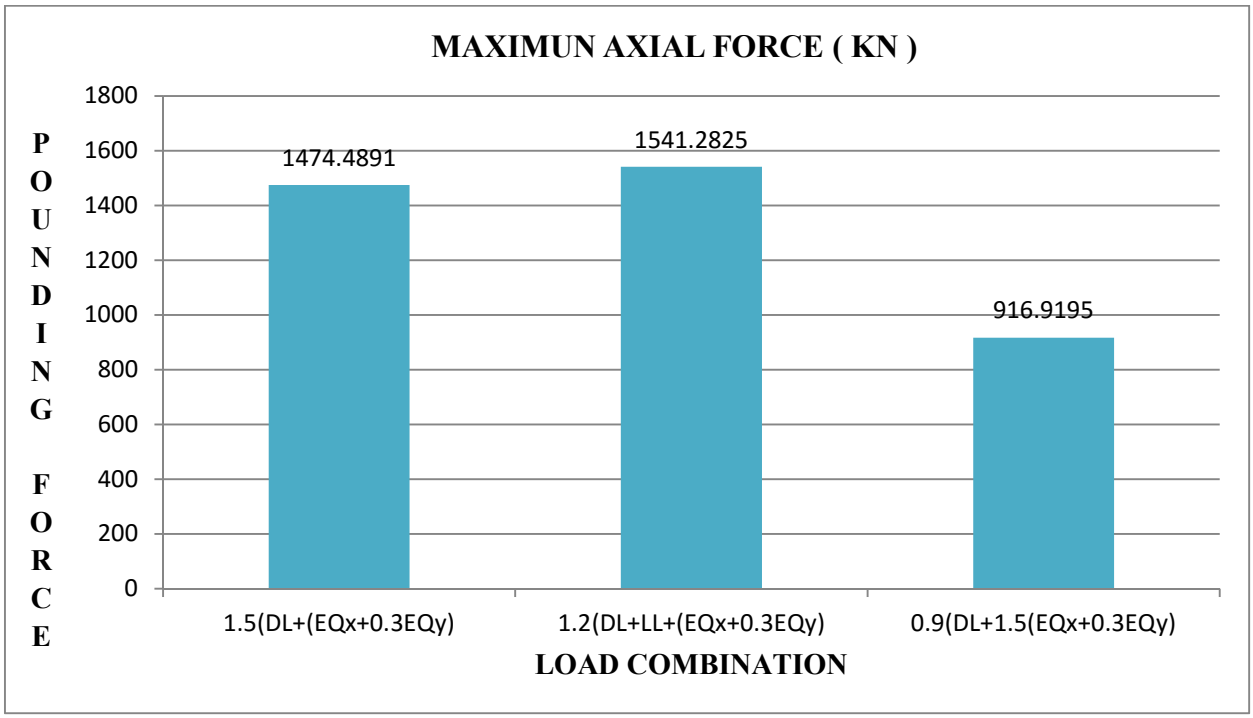

Figure 19: Maximum Axial force model 4

5.2.5 Comparison of Maximum Axial force for all models

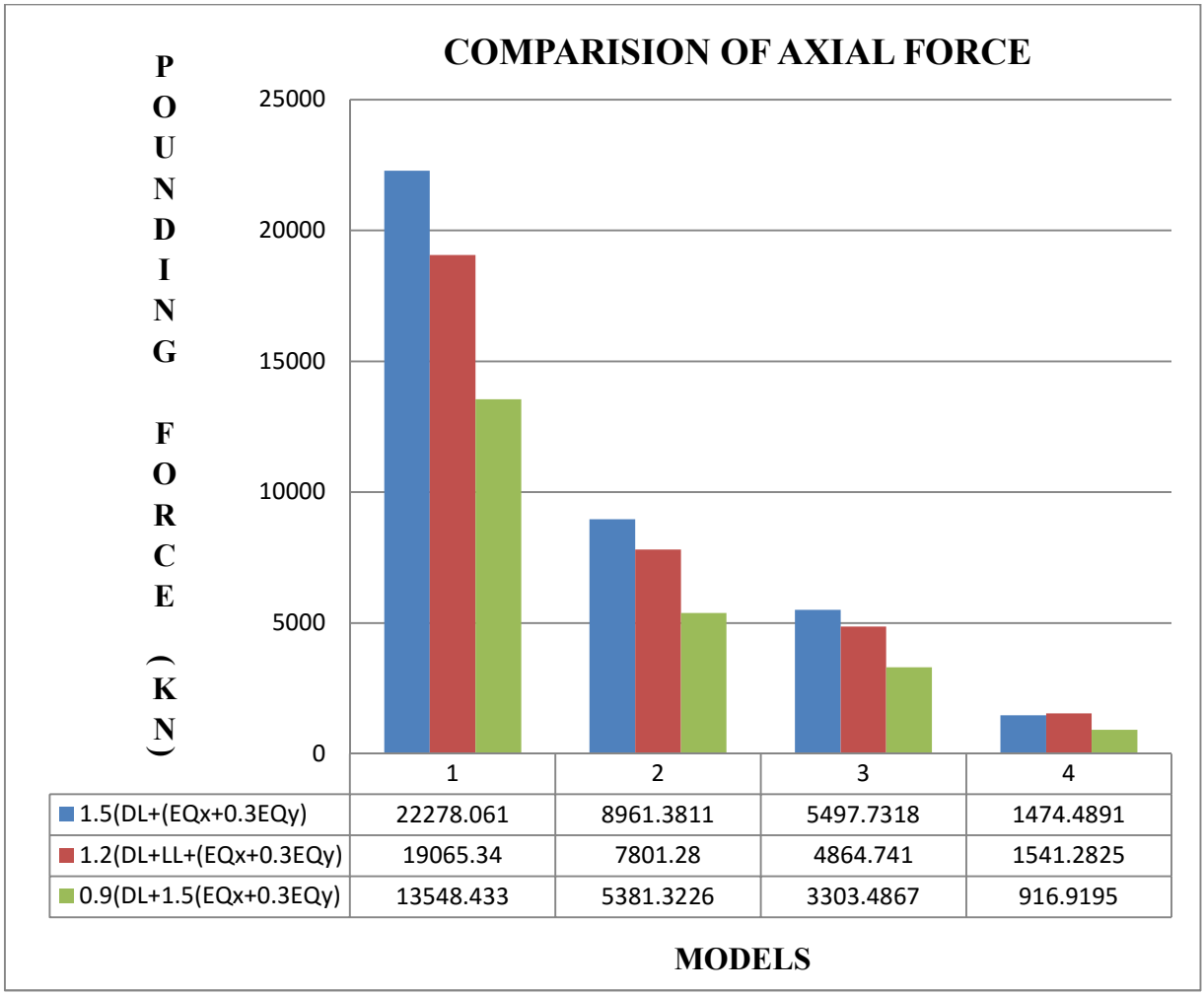

Figure 20: Comparison of Maximum Axial force for all models

Figure 20 shows comparison of maximum axial force for all four models. Here in this figure 20 model 1 (without stiffness in expansion joint) has maximum axial force of 22278.78 KN. Model 2 (lead rubber bearing in expansion joint) has maximum axial force of 8961.3811 which is less than model 1. Model 3 (rubber isolator in expansion joint) has maximum axial force of 5497.7318 KN which is less as compare to model 1 and model 2. Model 4 (high damping rubber bearing in expansion joint) has maximum axial force of 1541.2825 KN which is very less as compare to all three load cases. So from the comparison of axial force we obtain that high damping rubber bearing has very high resistance to pounding force and can be used in expansion joint for future design.

5.3 Maximum Moments of models

In this section of thesis maximum moment is calculated from analysis of all four models. Moment represents the bending due to axial force in the bridge. High moment can result in collision of bridge deck and could result in damage to bridge. So all the critical or maximum moments were compared to obtain best suited model.

5.3.1 Maximum moment of model 1

After analysing model 1 (without stiffness in expansion joint) all moment for three different load combinations are obtained. For load case 1 moment is 403328.7 KNm, for load case 2 moment is 347224.4 KNm and for load case 3 moment obtain is 242255.51 KN. Maximum moment for model 1 is given in table 29

Table 29: Maximum moment model 1

LOAD COMBINATION	MOMENT (KNm)
1.5(DL+(EQx+0.3EQy)	403328.7
1.2(DL+LL+(EQx+0.3EQy)	347224.4
0.9(DL+1.5(EQx+0.3EQy)	242255.5

As shown in figure 21 moments are shown in y axis and load cases are in x axis. Maximum moment for load case1 is much higher than load case 2 and 3. So load case 1 is most critical for model 1 (without stiffness in expansion joint).

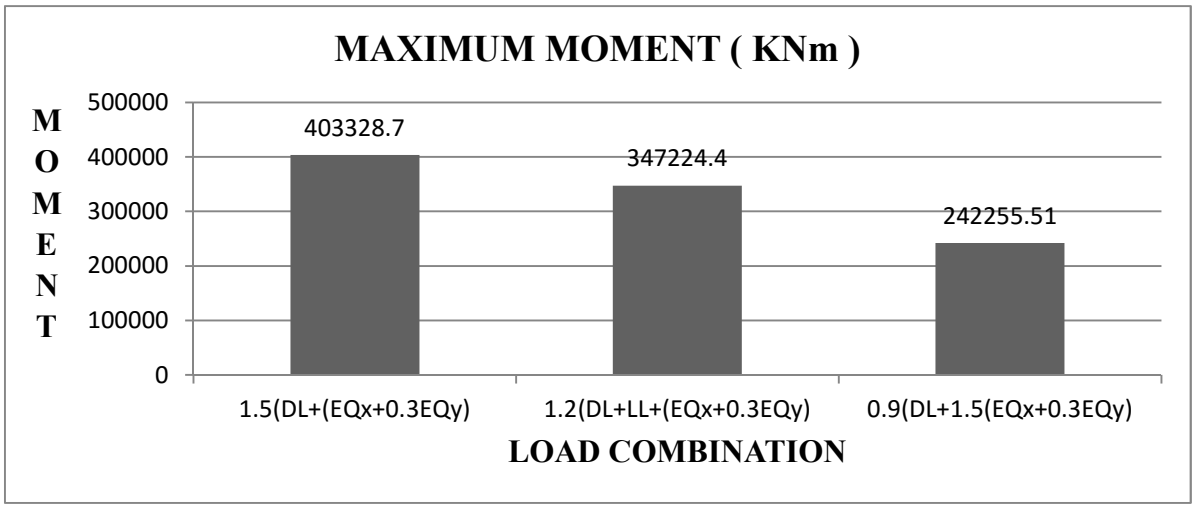

Figure 21: Maximum Moment model 1

5.3.2 Maximum moment model 2

In this model 2 lead rubber bearing is being provided to overcome the pounding force. After analysing the model 2 lead rubber bearing for all three load cases we obtain that load case 1 has maximum moment of 70139.29 KNm and load case 2 has moment of 61202.94 KNm. Similarly for load case 3 has maximum axial force of 42155.08 KNm. Maximum moment for model 2 is given in table 30

Table 30: Maximum moment model 2

LOAD COMBINATION	MOMENT (KNm)
1.5(DL+(EQx+0.3EQy)	70139.29
1.2(DL+LL+(EQx+0.3EQy)	61202.94
0.9(DL+1.5(EQx+0.3EQy)	42155.08

As shown in figure 22 moments are shown in y axis and load cases are in x axis. Maximum moment for load case1 is much higher than load case 2 and 3. So load case 1 is most critical for model 2 (lead rubber bearing in expansion joint).

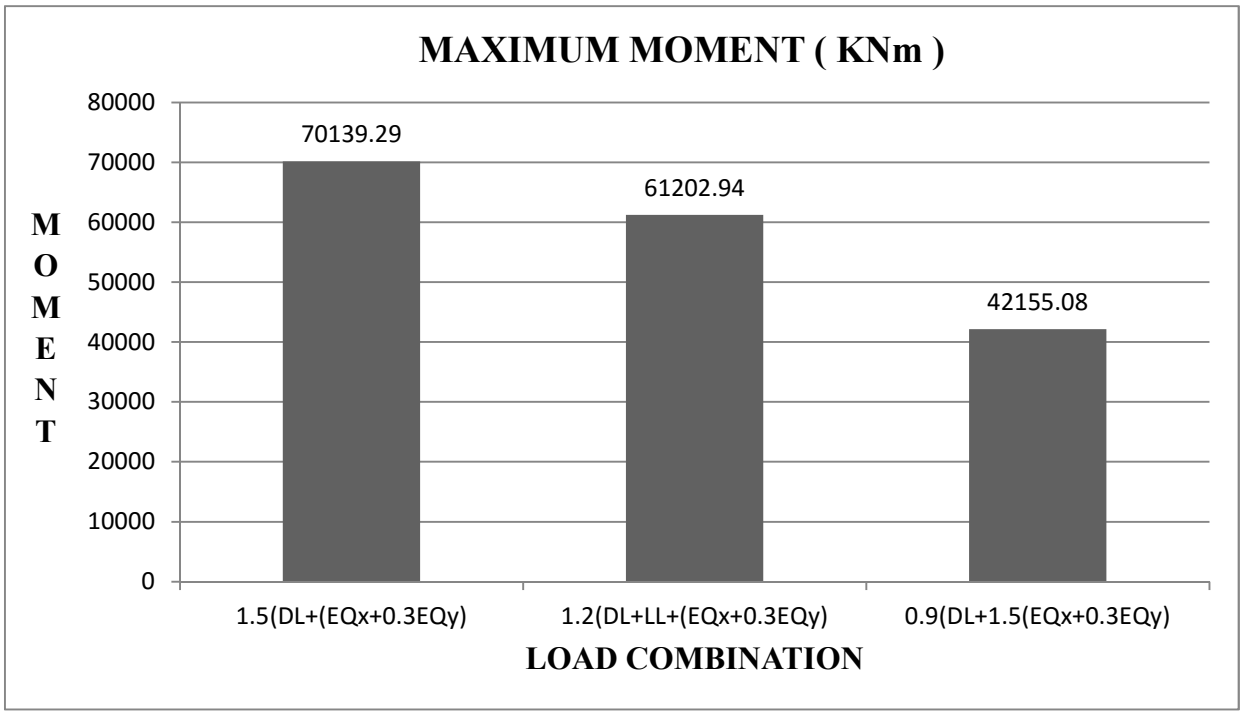

Figure 22: Maximum Moment model 2

5.3.3 Maximum moment model 3

In this model 3 rubber isolator bearing is being provided to overcome the pounding force. After analysing the model 3 rubber isolator bearing for all three load cases we obtain that load case 1 has maximum moment of 45485.81 KNm and load case 2 has moment of 40280.11 KNm. Similarly for load case 3 has maximum axial force of 27362.451 KNm. Maximum moment for model 3 is given in table 31

Table 31: Maximum moment model 3

LOAD COMBINATION	MOMENT (KNm)
1.5(DL+(EQx+0.3EQy)	45485.81
1.2(DL+LL+(EQx+0.3EQy)	40280.11
0.9(DL+1.5(EQx+0.3EQy)	27362.451

As shown in figure 23 moments are shown in y axis and load cases are in x axis. Maximum moment for load case1 is much higher than load case 2 and 3. So load case 1 is most critical for model 3 (rubber isolator bearing in expansion joint).

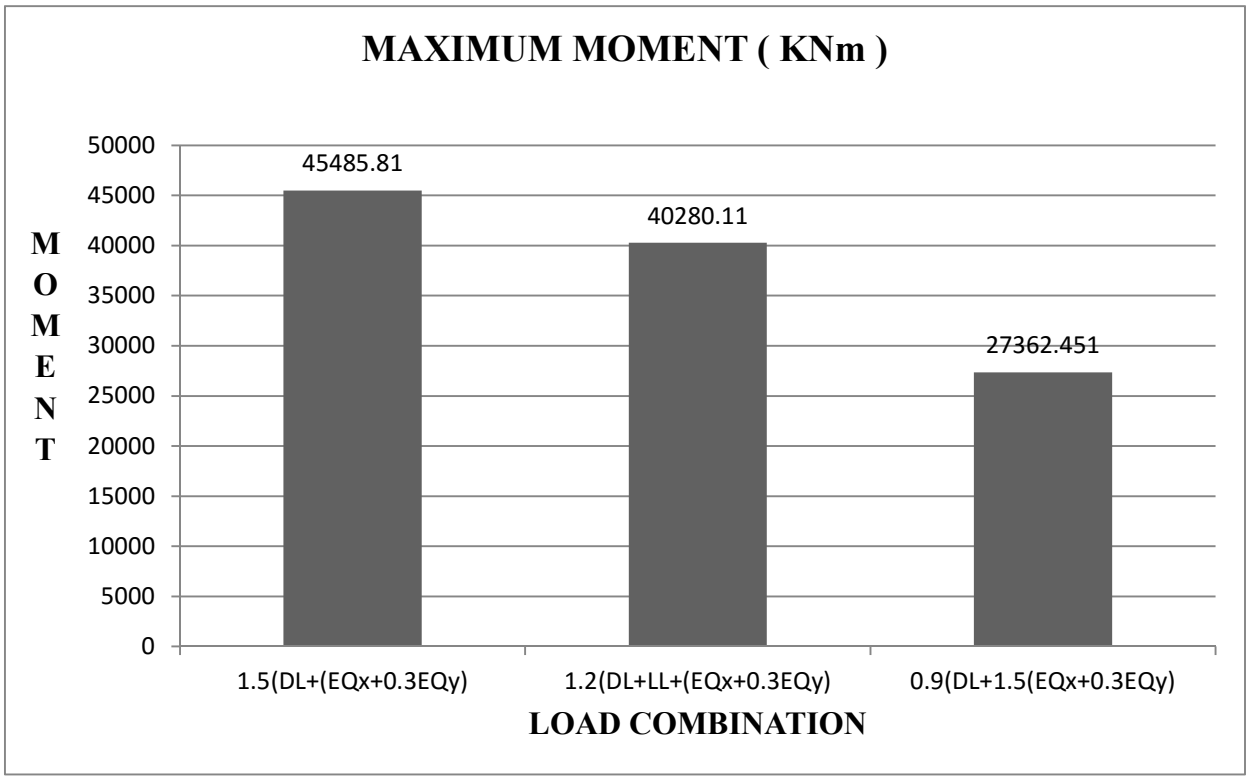

Figure: 23 Maximum Moment model 3

5.3.3 Maximum moment model 4

In this model 4 high damping rubber bearing is being provided to overcome the pounding force. After analysing the model 4 high damping rubber bearing bearing for all three load cases we obtain that load case 1 has maximum moment of 13857.099 KNm and load case 2 has moment of 14270.908 KNm. Similarly for load case 3 has maximum axial force of 8356.2722 KNm. Maximum moment for model 4 is given in table 32

Table 32: Maximum moment model 4

LOAD COMBINATION	MOMENT (KNm)
1.5(DL+(EQx+0.3EQy)	13857.099
1.2(DL+LL+(EQx+0.3EQy)	14270.908
0.9(DL+1.5(EQx+0.3EQy)	8356.2722

As shown in figure 24 moments are shown in y axis and load cases are in x axis. Maximum moment for load case1 is much higher than load case 2 and 3. So load case 1 is most critical for model 4 (high damping rubber bearing in expansion joint).

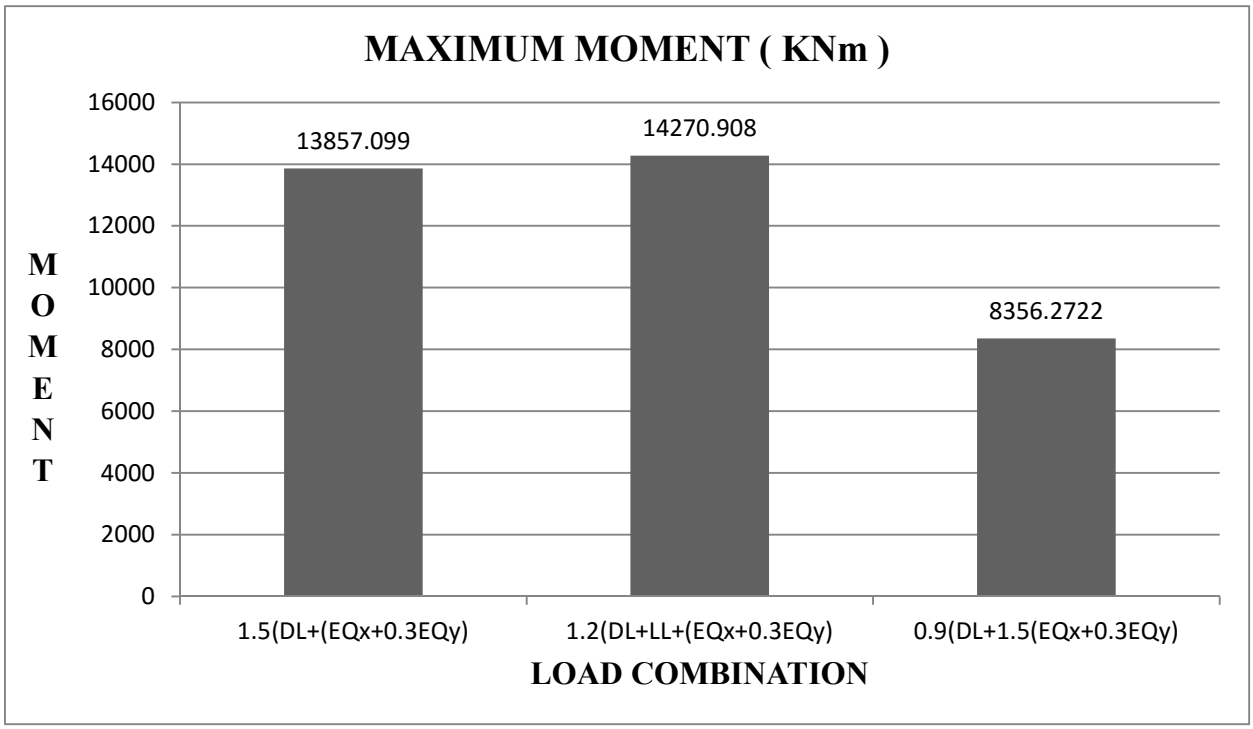

Figure 24: Maximum Moment model 4

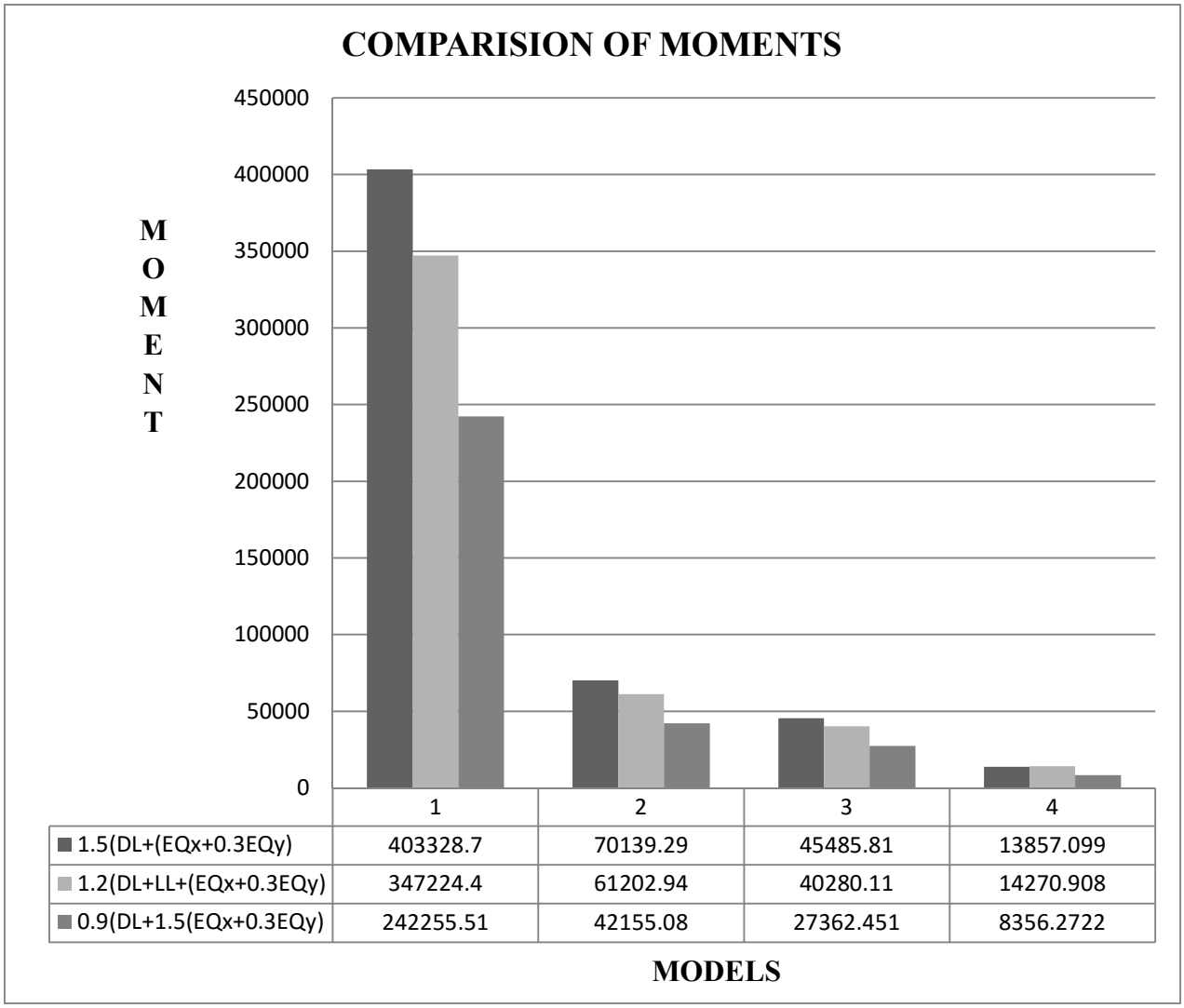

Figure 25: Comparison of Maximum Moment for all models

Figure 25 shows comparison of maximum moment for all four models. Here in this figure 25 model 1 (without stiffness in expansion joint) has maximum moment of 403328.7 KNm. Model 2 (lead rubber bearing in expansion joint) has maximum moment of 70139.29 KNm which is less than model 1. Model 3 (rubber isolator in expansion joint) has maximum moment of 45485.81 KNm which is less as compare to model 1 and model 2. Model 4 (high damping rubber bearing in expansion joint) has maximum moment of 13857.099 KNm which is very less as compare to all three load cases. So from the comparison of moment we obtain that high damping rubber bearing has very high resistance to pounding force and can be used in expansion joint for future design.

5.4 Maximum Stress at Top of models

In this section of thesis maximum stress at top is calculated from analysis of all four models. High stress at top can result in collision of bridge deck and could result in damage to bridge. So all the critical or Maximum stress at top were compared to obtain best suited model.

5.4.1 Maximum stress at top of model 1

After analysing model 1 (without stiffness in expansion joint) all stress at top for three different load combinations are obtained. For load case 1 stress at top is 309964.61 KN/m^2, for load case 2 stress at top is 261577.87 KN/m^2 and for load case 3 stress at top obtain is192991.84 KN/m^2. Maximum stress at top for model 1 is given in table 33

Table 33: Maximum stress at top model 1

LOAD COMBINATION	STRESS (KN/m^2)
1.5(DL+(EQx+0.3EQy)	309964.61
1.2(DL+LL+(EQx+0.3EQy)	261577.87
0.9(DL+1.5(EQx+0.3EQy)	192991.84

As shown in figure 26 stress at top are shown in y axis and load cases are in x axis. Maximum stress at top for load case1 is much higher than load case 2 and 3. So load case 1 is most critical for model 1 (without stiffness in expansion joint).

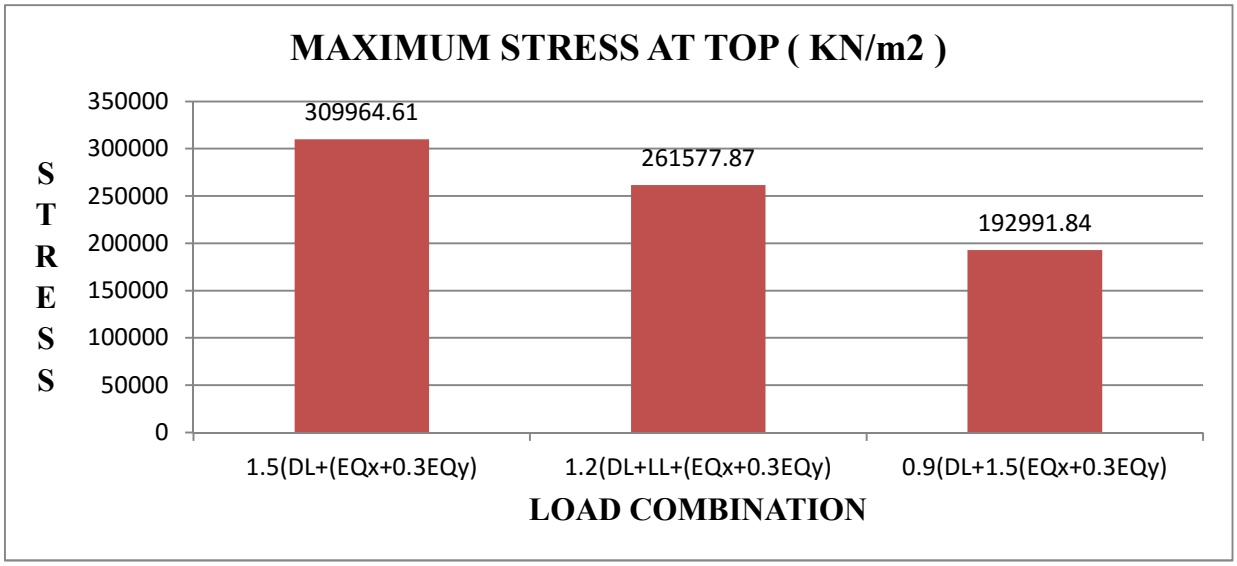

Figure 26: Maximum Stress at Top model 1

5.4.2 Maximum stress at top of model 2

After analysing model 2 (lead rubber bearing in expansion joint) all stress at top for three different load combinations are obtained. For load case 1 stress at top is 36494.5KN/m^2, for load case 2 stress at top is 32495.81 KN/m^2 and for load case 3 stress at top obtain is 21996.284KN/m^2. Maximum stress at top for model 2 is given in table 34

Table 34: Maximum stress at top model 2

LOAD COMBINATION	STRESS (KN/m^2)
1.5(DL+(EQx+0.3EQy)	36494.5
1.2(DL+LL+(EQx+0.3EQy)	32495.81
0.9(DL+1.5(EQx+0.3EQy)	21996.284

As shown in figure 27 stress at top are shown in y axis and load cases are in x axis. Maximum stress at top for load case1 is much higher than load case 2 and 3. So load case 1 is most critical for model 2 (lead rubber bearing in expansion joint).

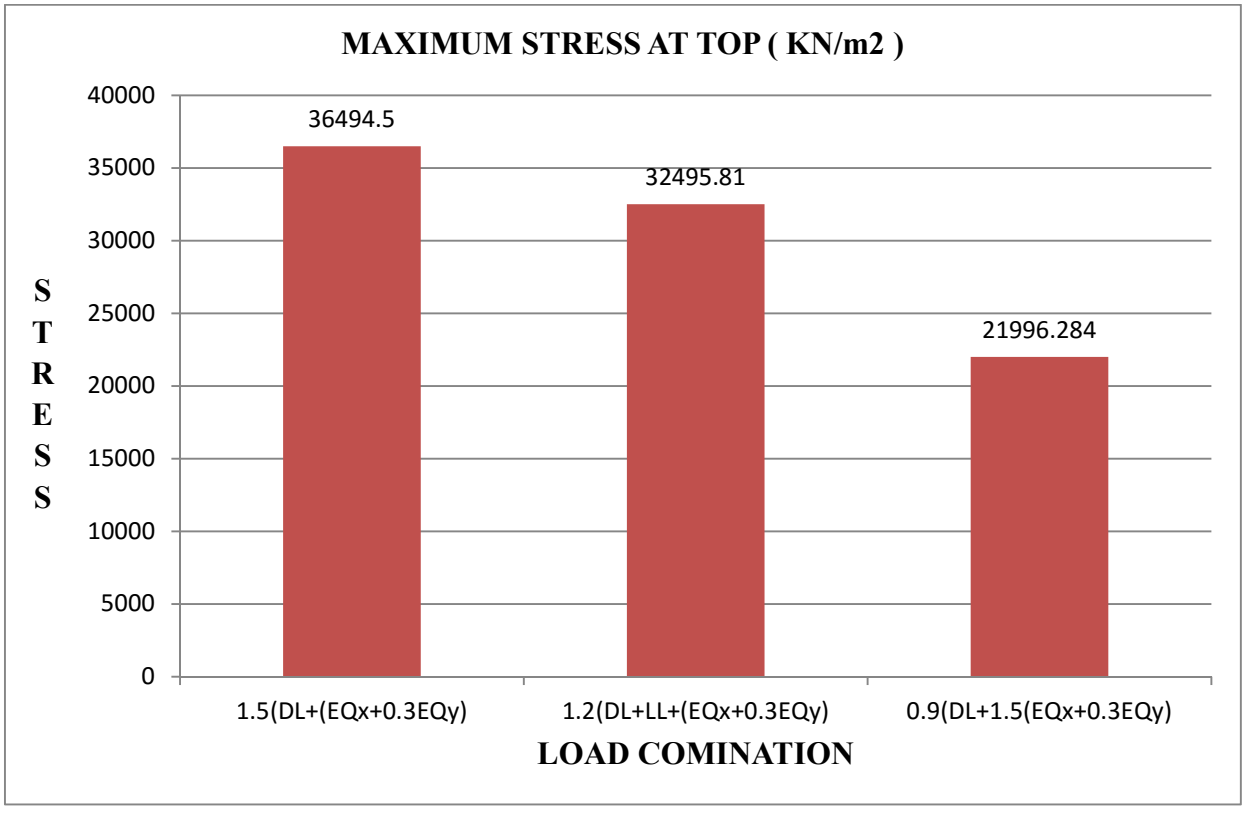

Figure 27: Maximum Stress at Top model 2

5.4.3 Maximum stress at top of model 3

After analysing model 3 (rubber isolator in expansion joint) all stress at top for three different load combinations are obtained. For load case 1 stress at top is 21974.984 KN/m^2, for load case 2 stress at top is 20707.258 KN/m^2 and for load case 3 stress at top obtain is 13283.023 KN/m^2. Maximum stress at top for model 3 is given in table 35

Table 35: Maximum stress at top model 3

LOAD COMBINATION	STRESS (KN/m^2)
1.5(DL+(EQx+0.3EQy)	21974.984
1.2(DL+LL+(EQx+0.3EQy)	20707.258
0.9(DL+1.5(EQx+0.3EQy)	13283.023

As shown in figure 28 stress at top are shown in y axis and load cases are in x axis. Maximum stress at top for load case1 is much higher than load case 2 and 3. So load case 1 is most critical for model 3 (rubber isolator bearing in expansion joint).

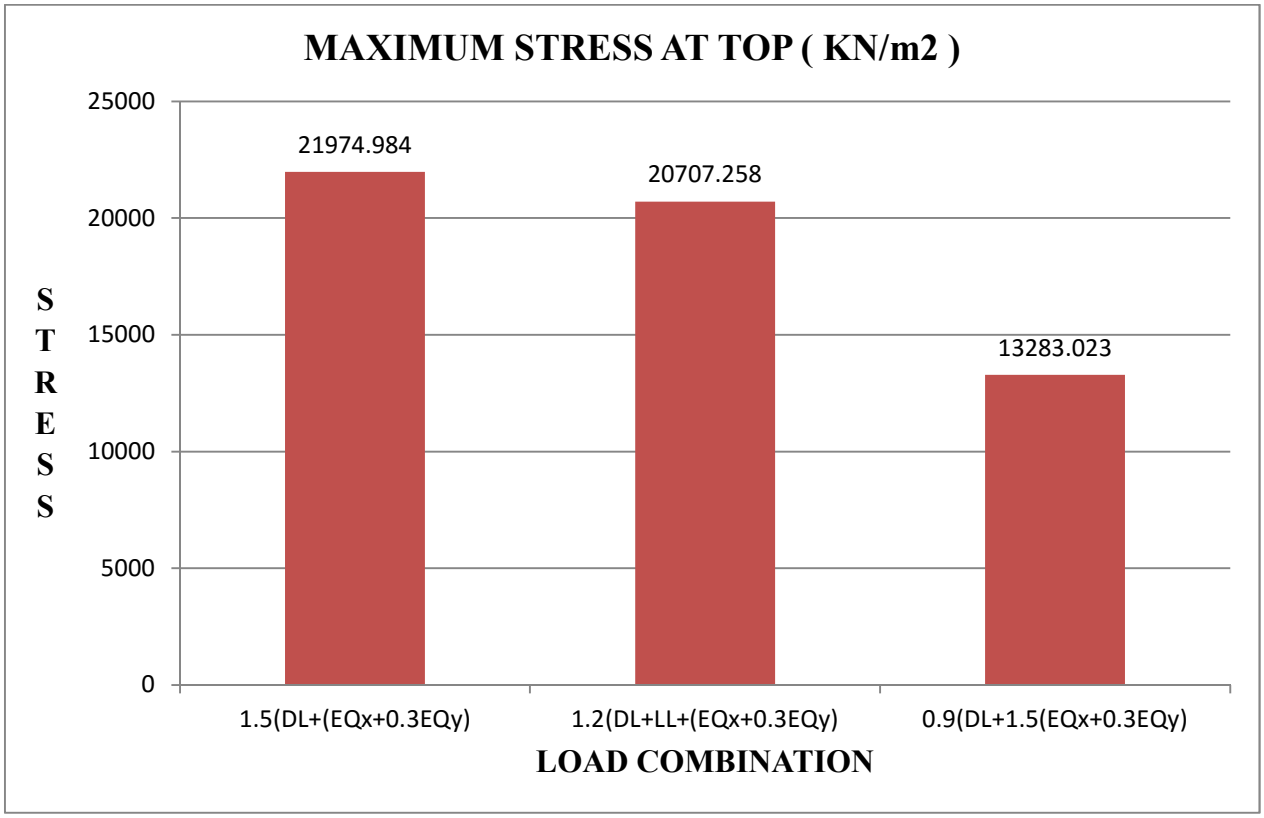

Figure 28: Maximum Stress at Top model 3

5.4.4 Maximum stress at top of model 4

After analysing model 4 (high damping rubber isolator in expansion joint) all stress at top for three different load combinations are obtained. For load case 1 stress at top is 9567.6603 KN/m^2, for load case 2 stress at top is 10659.01 KN/m^2 and for load case 3 stress at top obtain is 5816.5916 KN/m^2. Maximum stress at top for model 4 is given in table 36

Table 36: Maximum stress at top model 4

LOAD COMBINATION	STRESS (KN/m^2)
1.5(DL+(EQx+0.3EQy)	9567.6603
1.2(DL+LL+(EQx+0.3EQy)	10659.01
0.9(DL+1.5(EQx+0.3EQy)	5816.5916

As shown in figure 29 stress at top are shown in y axis and load cases are in x axis. Maximum stress at top for load case1 is much higher than load case 2 and 3. So load case 1 is most critical for model 4 (high damping rubber bearing in expansion joint)

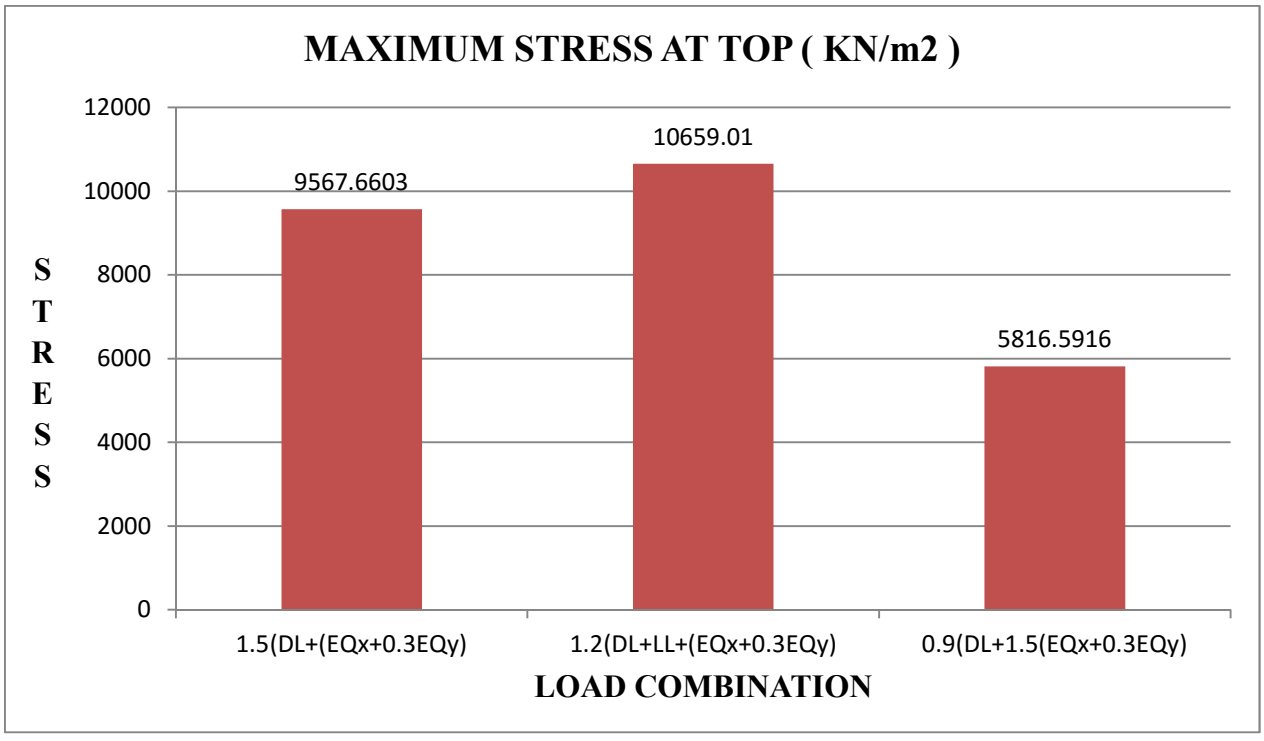

Figure 29: Maximum Stress at Top model

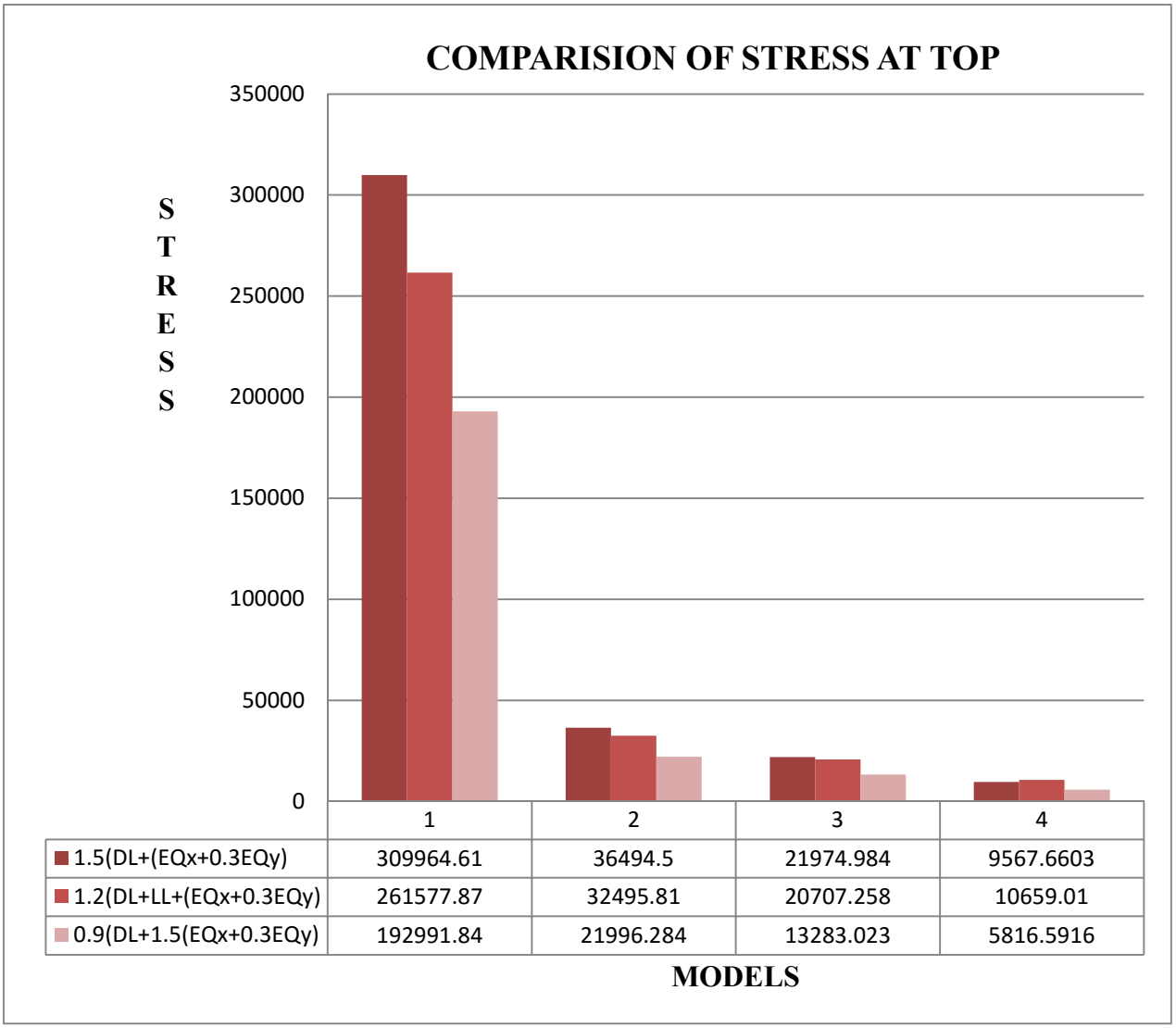

Figure 30: Comparison of Maximum Stress at Top for all models

Figure 30 shows comparison of maximum stress at top for all four models. Here in this figure 30 model 1 (without stiffness in expansion joint) has maximum stress at top of 309964.61KN/m^2. Model 2 (lead rubber bearing in expansion joint) has maximum stress at top of 36494.5 KN/m^2 which is less than model 1. Model 3 (rubber isolator in expansion joint) has maximum stress at top of 21974.984 KN/m^2 which is less as compare to model 1 and model 2. Model 4 (high damping rubber bearing in expansion joint) has maximum stress at top of 10659.01 KN/m^2 which is very less as compare to all three load cases. So from the comparison of maximum stress at top we obtain that high damping rubber bearing has very high resistance to pounding force and can be used in expansion joint for future design.

5.5 Maximum Stress at Bottom of models

In this section of thesis maximum stress at bottom is calculated from analysis of all four models. High stress at bottom can result in collision of bridge deck and could result in damage to bridge. So all the critical or maximum stress at bottom were compared to obtain best suited model.

5.5.1 Maximum stress at bottom of model 1

After analysing model 1 (without stiffness in expansion joint) all stress at bottom for three different load combinations are obtained. For load case 1 stress at bottom is 129991.18 KN/m^2, for load case 2 stress at bottom is 111870.74 KN/m^2 and for load case 3 stress at bottom obtain is 78279.63KN/m^2. Maximum stress at bottom for model 1 is given in table 37

Table 37: Maximum stress at bottom model 1

LOAD COMBINATION	STRESS (KN/m^2)
1.5(DL+(EQx+0.3EQy)	129991.18
1.2(DL+LL+(EQx+0.3EQy)	111870.74
0.9(DL+1.5(EQx+0.3EQy)	78279.63

As shown in figure 31 stress at bottom are shown in y axis and load cases are in x axis. Maximum stress at bottom for load case1 is much higher than load case 2 and 3. So load case 1 is most critical for model 1 (without stiffness in expansion joint).

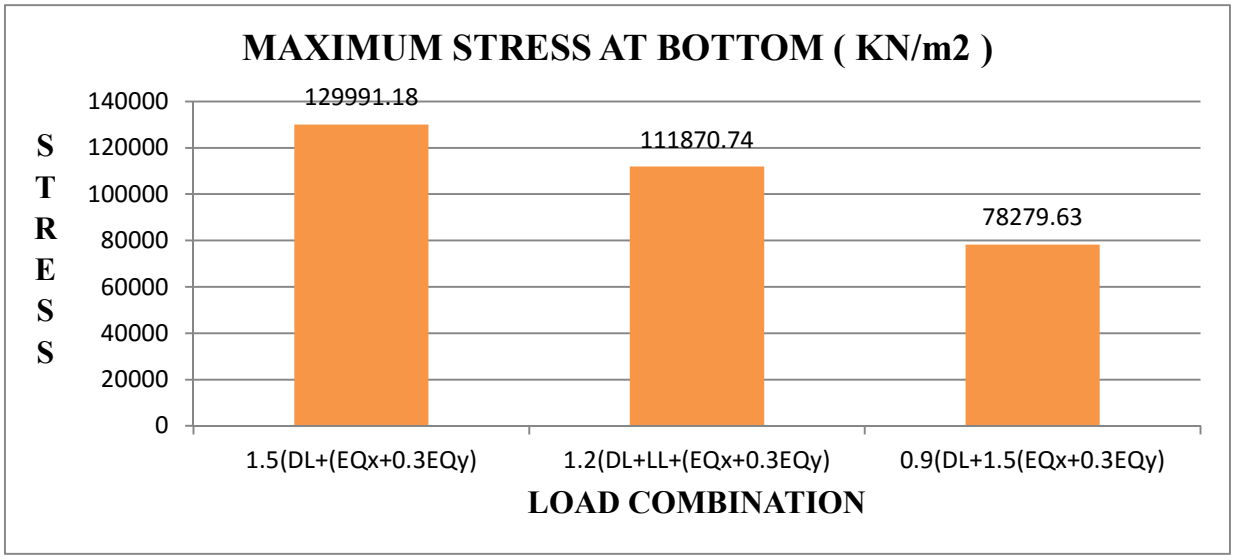

Figure 31: Maximum Stress at Bottom model 1

5.5.2 Maximum stress at bottom of model 2

After analysing model 2 (lead rubber bearing in expansion joint) all stress at bottom for three different load combinations are obtained. For load case 1 stress at bottom is 22593.14KN/m^2, for load case 2 stress at bottom is 19714.14 KN/m^2 and for load case 3 stress at bottom obtain is 13590.884 KN/m^2. Maximum stress at bottom for model 2 is given in table 38

Table 38: Maximum stress at top model 2

LOAD COMBINATION	STRESS (KN/m^2)
1.5(DL+(EQx+0.3EQy)	22593.14
1.2(DL+LL+(EQx+0.3EQy)	19714.14
0.9(DL+1.5(EQx+0.3EQy)	13590.884

As shown in figure 32 stress at bottom are shown in y axis and load cases are in x axis. Maximum stress at bottom for load case1 is much higher than load case 2 and 3. So load case 1 is most critical for model 2 (lead rubber bearing in expansion joint).

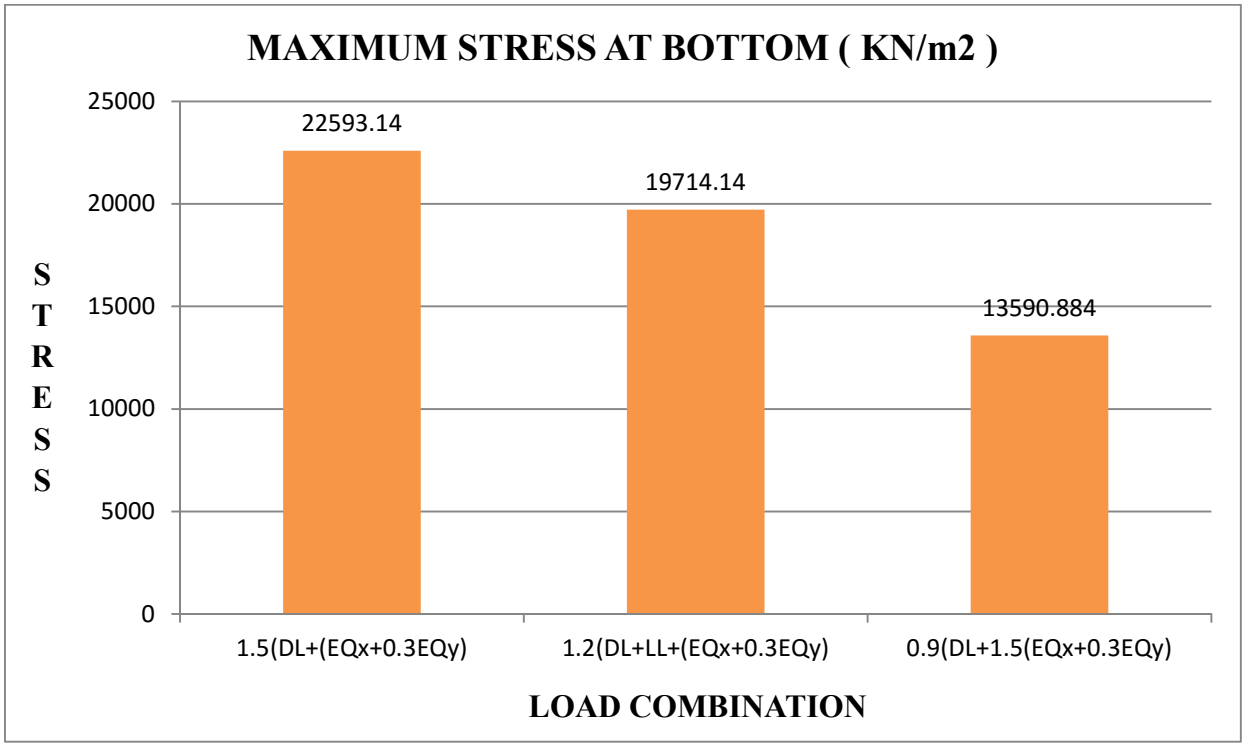

Figure 32: Maximum Stress at Bottom model 2

5.5.3 Maximum stress at bottom of model 3

After analysing model 3 (rubber isolator bearing in expansion joint) all stress at bottom for three different load combinations are obtained. For load case 1 stress at bottom is 14631.046 KN/m^2, for load case 2 stress at bottom is 12954.925 KN/m^2 and for load case 3 stress at bottom obtain is 8810.6542 KN/m^2. Maximum stress at bottom for model 3 is given in table 39

Table 39: Maximum stress at top model 3

LOAD COMBINATION	STRESS (KN/m^2)
1.5(DL+(EQx+0.3EQy)	14631.046
1.2(DL+LL+(EQx+0.3EQy)	12954.925
0.9(DL+1.5(EQx+0.3EQy)	8810.6542

As shown in figure 33 stress at bottom are shown in y axis and load cases are in x axis. Maximum stress at bottom for load case1 is much higher than load case 2 and 3. So load case 1 is most critical for model 3 (rubber isolator in expansion joint).

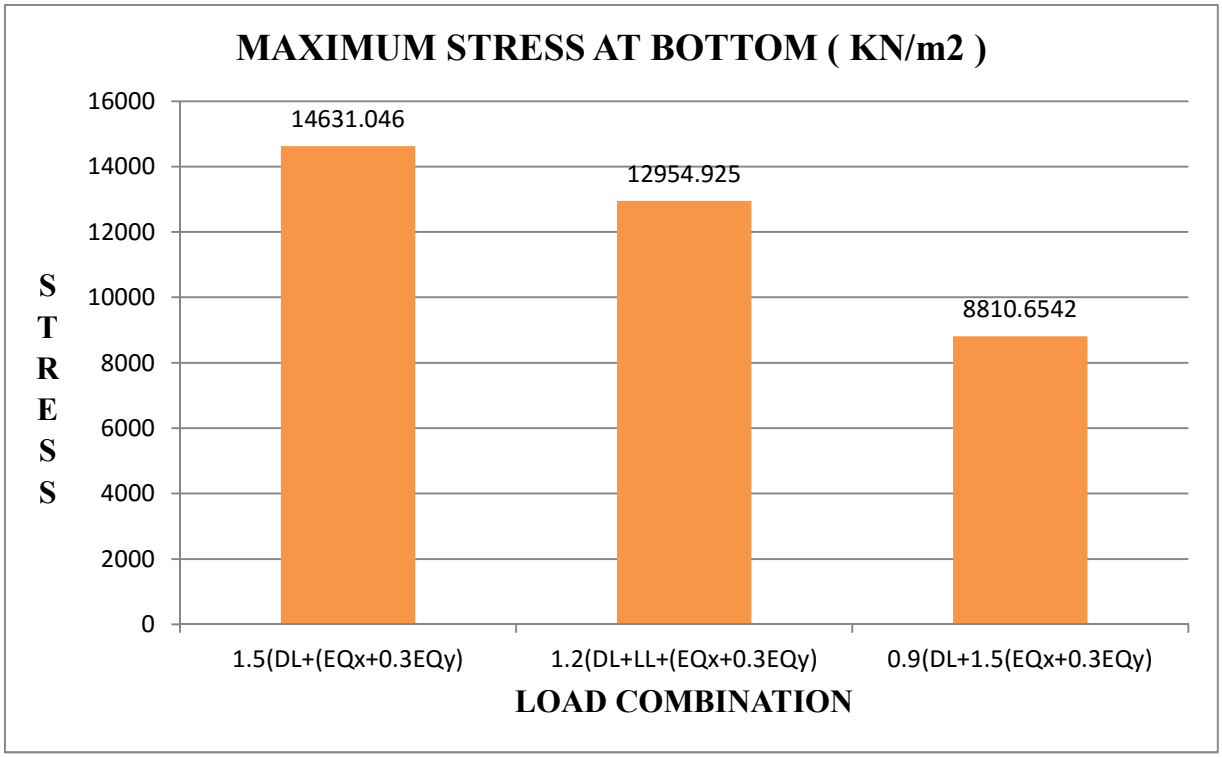

Figure 33: Maximum Stress at Bottom model 3

5.5.4 Maximum stress at bottom of model 4

After analysing model 4 (high damping rubber bearing in expansion joint) all stress at bottom for three different load combinations are obtained. For load case 1 stress at bottom is 4489.92 KN/m^2, for load case 2 stress at bottom is 4616.172 KN/m^2 and for load case 3 stress at bottom obtain is 2713.6694 KN/m^2. Maximum stress at bottom for model 4 is given in table 40

Table 40: Maximum stress at top model 4

LOAD COMBINATION	STRESS (KN/m^2)
1.5(DL+(EQx+0.3EQy)	4489.92
1.2(DL+LL+(EQx+0.3EQy)	4616.172
0.9(DL+1.5(EQx+0.3EQy)	2713.6694

As shown in figure 34 stress at bottom are shown in y axis and load cases are in x axis. Maximum stress at bottom for load case1 is much higher than load case 2 and 3. So load case 1 is most critical for model 4 (high damping rubber bearing in expansion joint).

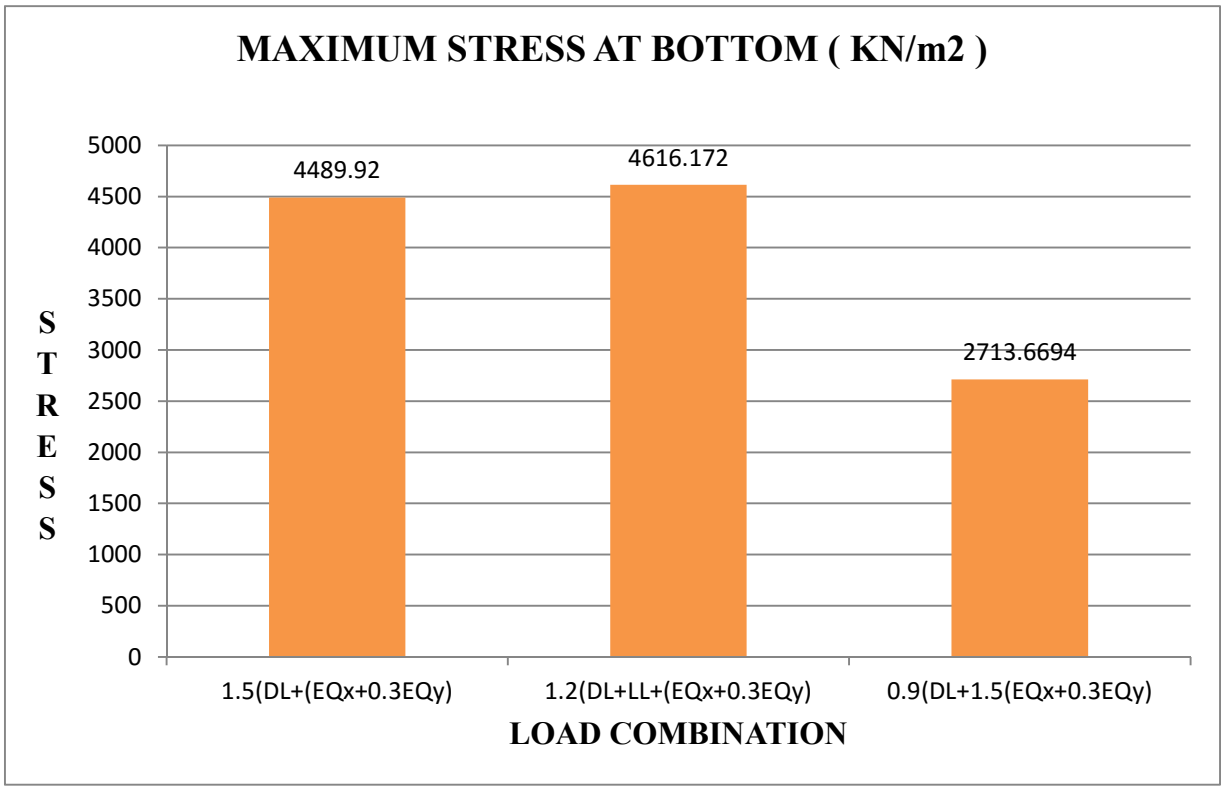

Figure 34: Maximum Stress at Bottom model 4

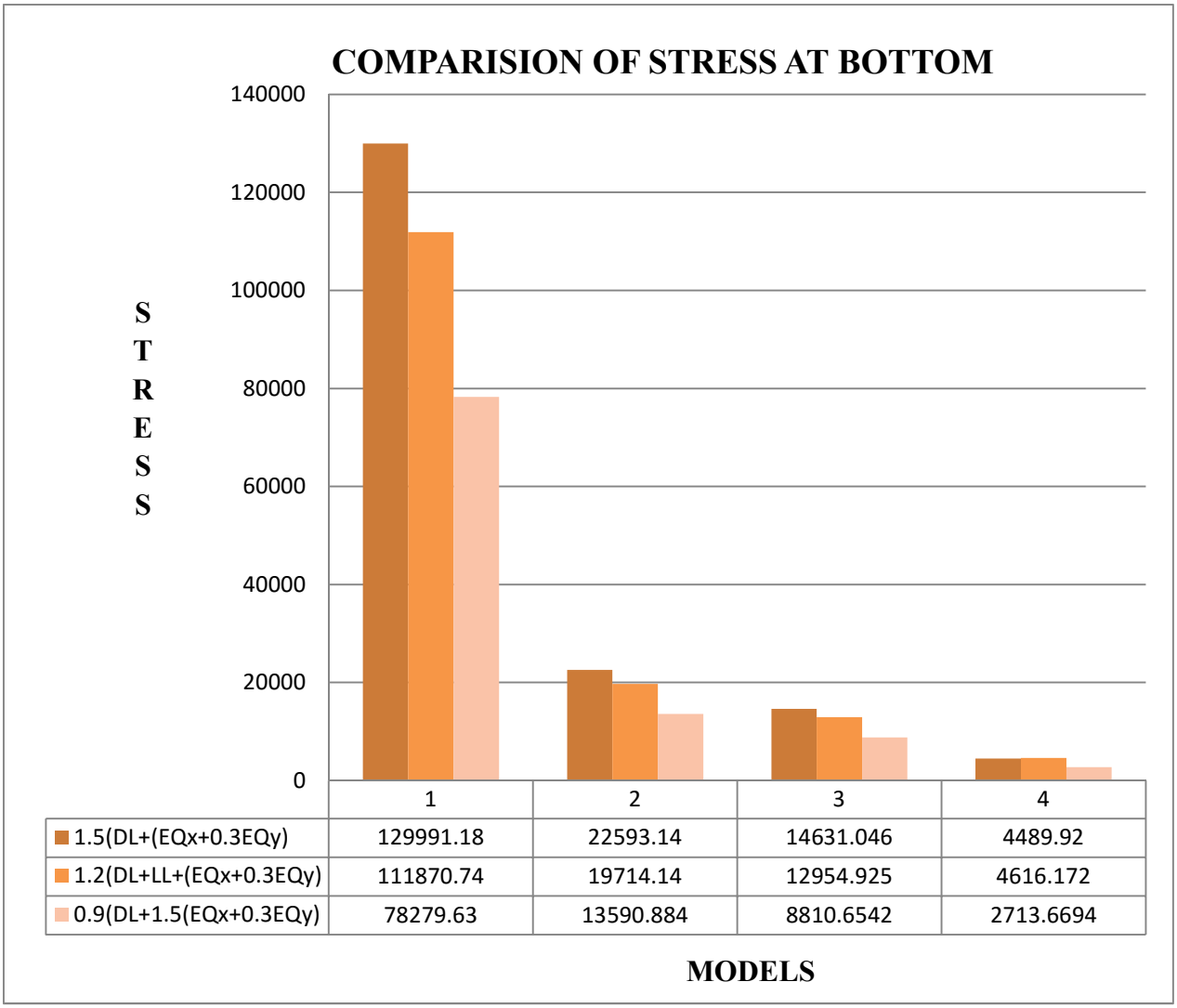

Figure 35: Comparison of Maximum Stress at Bottom for all models

Figure 35 shows comparison of maximum stress at bottom for all four models. Here in this figure 35 model 1 (without stiffness in expansion joint) has maximum stress at bottom of 129991.18 KN/m^2. Model 2 (lead rubber bearing in expansion joint) has maximum stress at bottom of 22593.14 KN/m^2 which is less than model 1. Model 3 (rubber isolator in expansion joint) has maximum stress at bottom of 14631.046 KN/m^2 which is less as compare to model 1 and model 2. Model 4 (high damping rubber bearing in expansion joint) has maximum stress at bottom of 4616.172 KN/m^2 which is very less as compare to all three load cases. So from the comparison of maximum stress at bottom we obtain that high damping rubber bearing has very high resistance to pounding force and can be used in expansion joint for future design.

5.6 Maximum Displacement of models

In this section of thesis maximum displacement is calculated from analysis of all four models. High displacement can result in collision of bridge deck and could result in damage to bridge. So all the critical or maximum displacement were compared to obtain best suited model.

5.6.1 Maximum displacement of model 1

After analysing model 1 (without stiffness in expansion joint) all displacement for three different load combinations are obtained. For load case 1 displacement is 0.6084 m, for load case 2 displacement is 0.5358 m and for load case 3 displacement obtain is 0.5087 m. Maximum displacement for model 1 is given in table 41

Table 41: Maximum Displacement model 1

LOAD COMBINATION	DISPLACEMENT (m)
1.5(DL+(EQx+0.3EQy)	0.6084
1.2(DL+LL+(EQx+0.3EQy)	0.5358
0.9(DL+1.5(EQx+0.3EQy)	0.5087

As shown in figure 36 displacement are shown in y axis and load cases are in x axis. Maximum displacement for load case1 is much higher than load case 2 and 3. So load case 1 is most critical for model 1 (without stiffness in expansion joint).

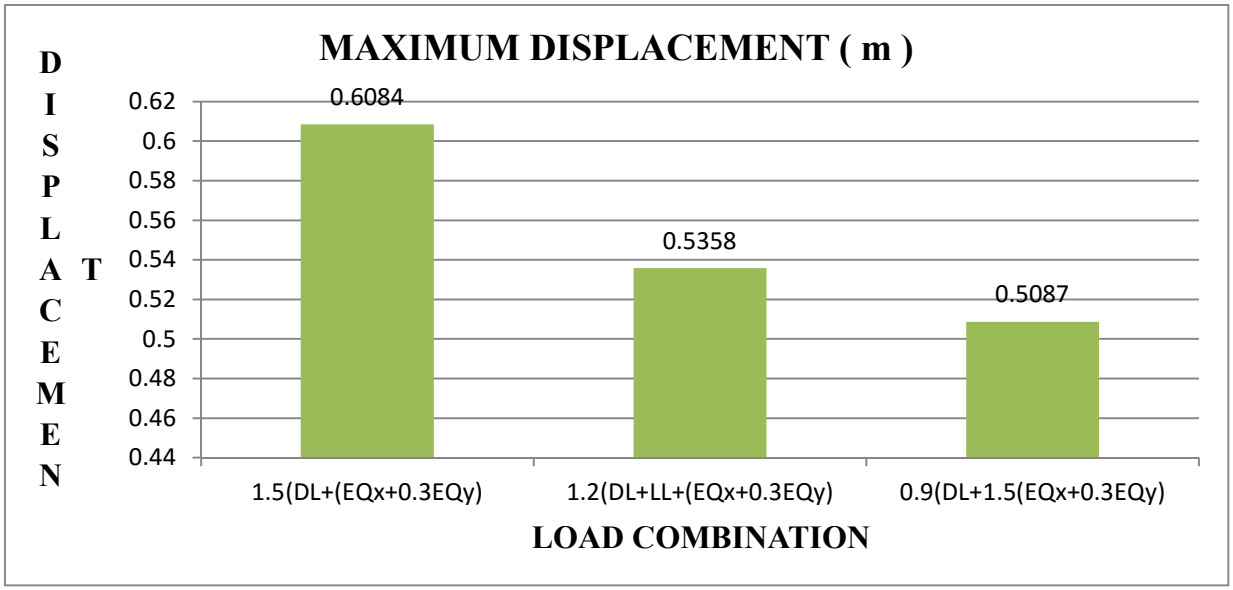

Figure 36: Maximum Displacement model 1

5.6.2 Maximum displacement of model 2

After analysing model 2 (lead rubber bearing in expansion joint) all displacement for three different load combinations are obtained. For load case 1 displacement is 0.5971 m, for load case 2 displacement is 0.4812 m and for load case 3 displacement obtain is 0.4034 m. Maximum displacement for model 2 is given in table 42

Table 42: Maximum displacement model 2

LOAD COMBINATION	DISPLACEMENT (m)
1.5(DL+(EQx+0.3EQy)	0.5971
1.2(DL+LL+(EQx+0.3EQy)	0.4812
0.9(DL+1.5(EQx+0.3EQy)	0.4034

As shown in figure 37 displacement are shown in y axis and load cases are in x axis. Maximum displacement for load case1 is much higher than load case 2 and 3. So load case 1 is most critical for model 2 (Lead Rubber Bearing in expansion joint).

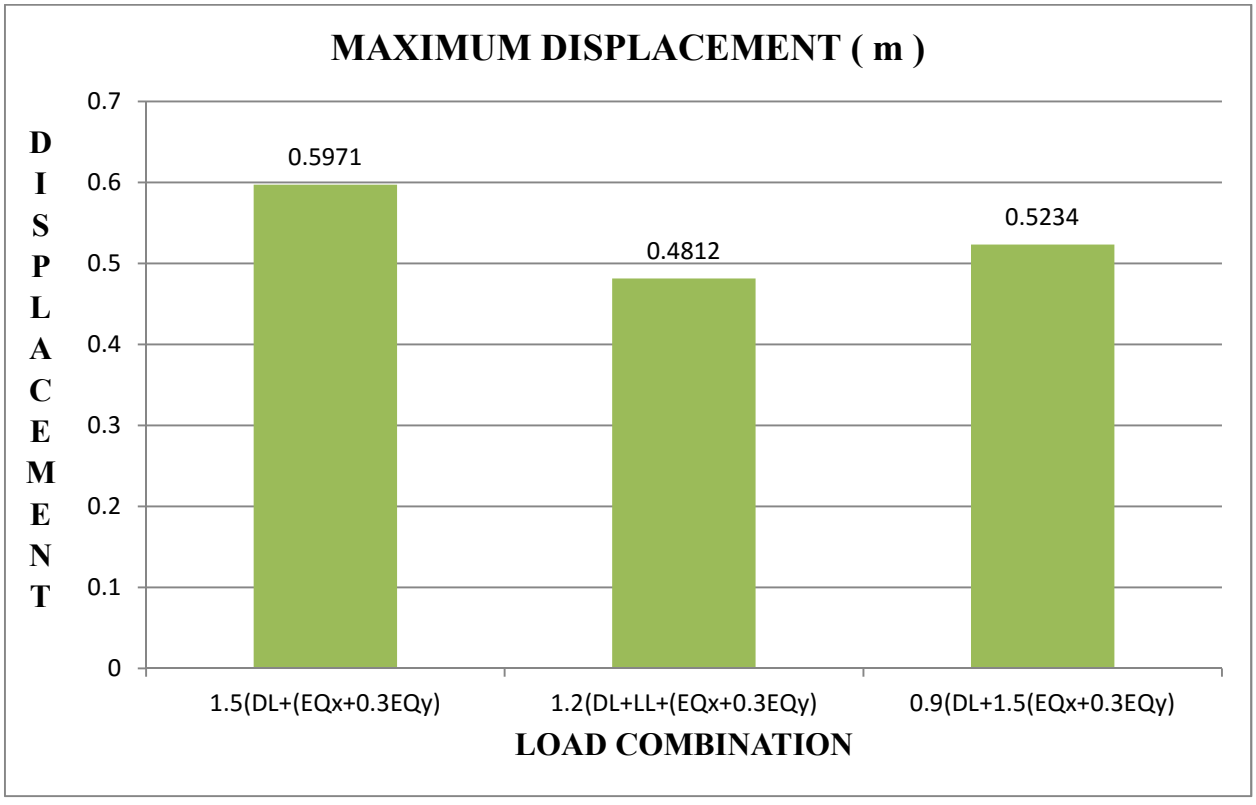

Figure 37: Maximum Displacement model 2

5.6.3 Maximum displacement of model 3

After analysing model 3 (rubber isolator in expansion joint) all displacement for three different load combinations are obtained. For load case 1 displacement is 0.2894 m, for load case 2 displacement is 0.2315 m and for load case 3 displacement obtain is 0.2309 m. Maximum displacement for model 3 is given in table 43

Table 43: Maximum displacement model 3

LOAD COMBINATION	DISPLACEMENT (m)
1.5(DL+(EQx+0.3EQy)	0.2894
1.2(DL+LL+(EQx+0.3EQy)	0.2315
0.9(DL+1.5(EQx+0.3EQy)	0.2309

As shown in figure 38 displacement are shown in y axis and load cases are in x axis. Maximum displacement for load case1 is much higher than load case 2 and 3. So load case 1 is most critical for model 3 (Rubber isolator in expansion joint).

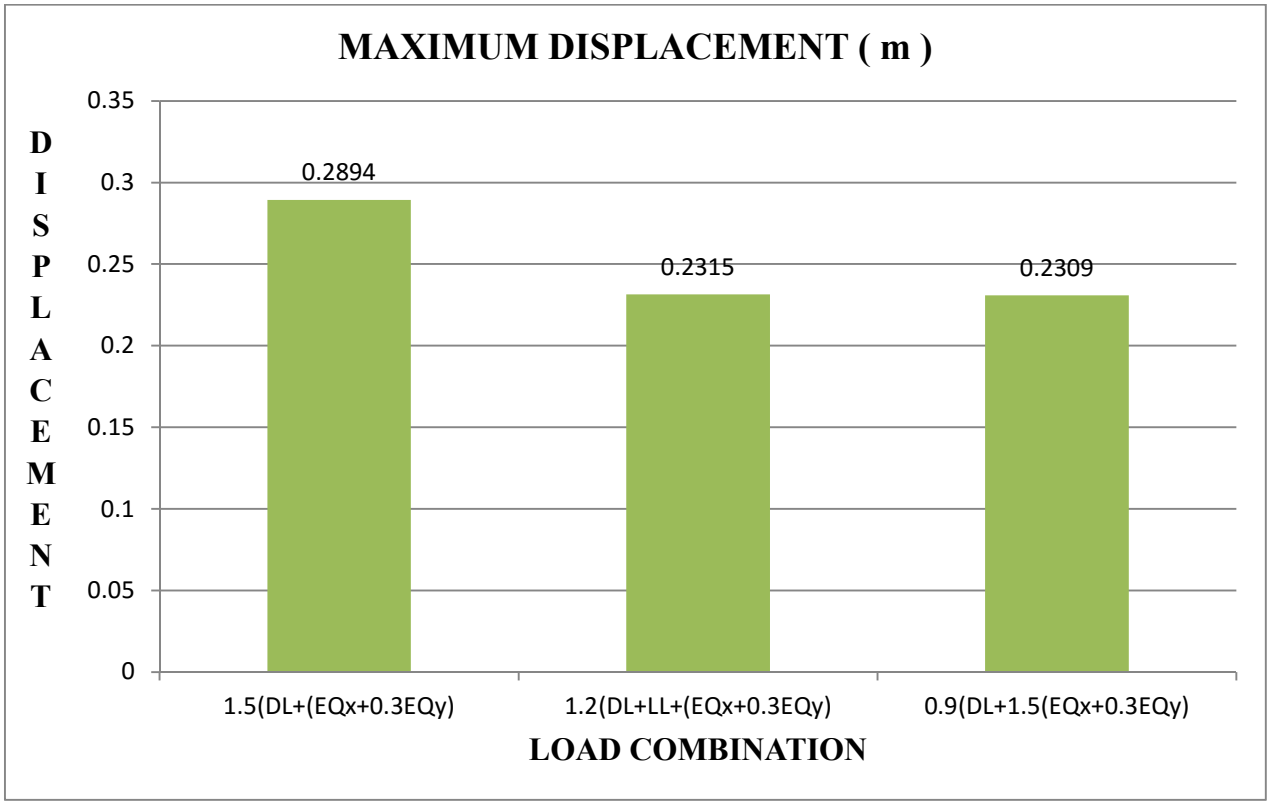

Figure 38: Maximum Displacement model 3

5.6.3 Maximum displacement of model 4

After analysing model 4 (high damping rubber bearing in expansion joint) all displacement for three different load combinations are obtained. For load case 1 displacement is 0.0594 m, for load case 2 displacement is 0.0496 m and for load case 3 displacement obtain is 0.0448 m. Maximum displacement for model 4 is given in table 44

Table 44: Maximum displacement model 4

LOAD COMBINATION	DISPLACEMENT (m)
1.5(DL+(EQx+0.3EQy)	0.0594
1.2(DL+LL+(EQx+0.3EQy)	0.0496
0.9(DL+1.5(EQx+0.3EQy)	0.0448

As shown in figure 39 displacement are shown in y axis and load cases are in x axis. Maximum displacement for load case1 is much higher than load case 2 and 3. So load case 1 is most critical for model 4 (High damping rubber bearing in expansion joint).

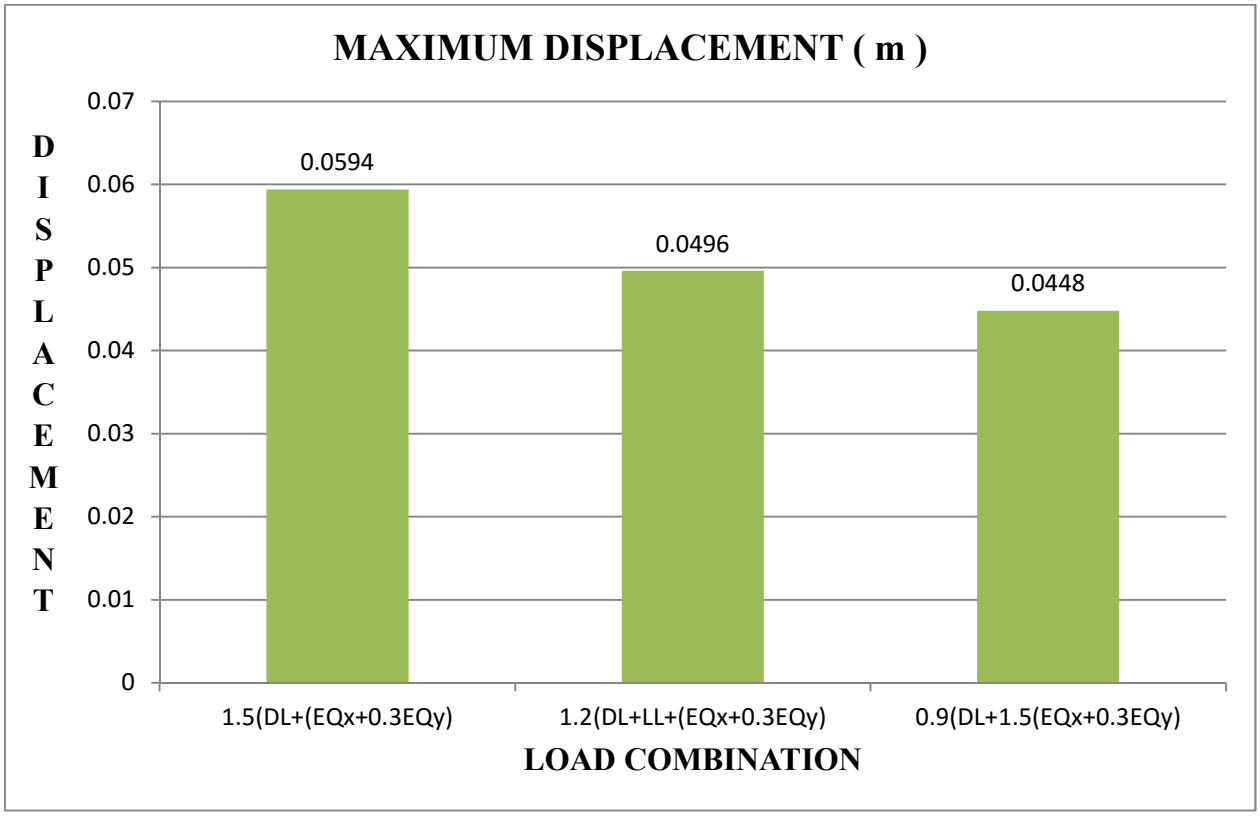

Figure 39: Maximum Displacement model 4

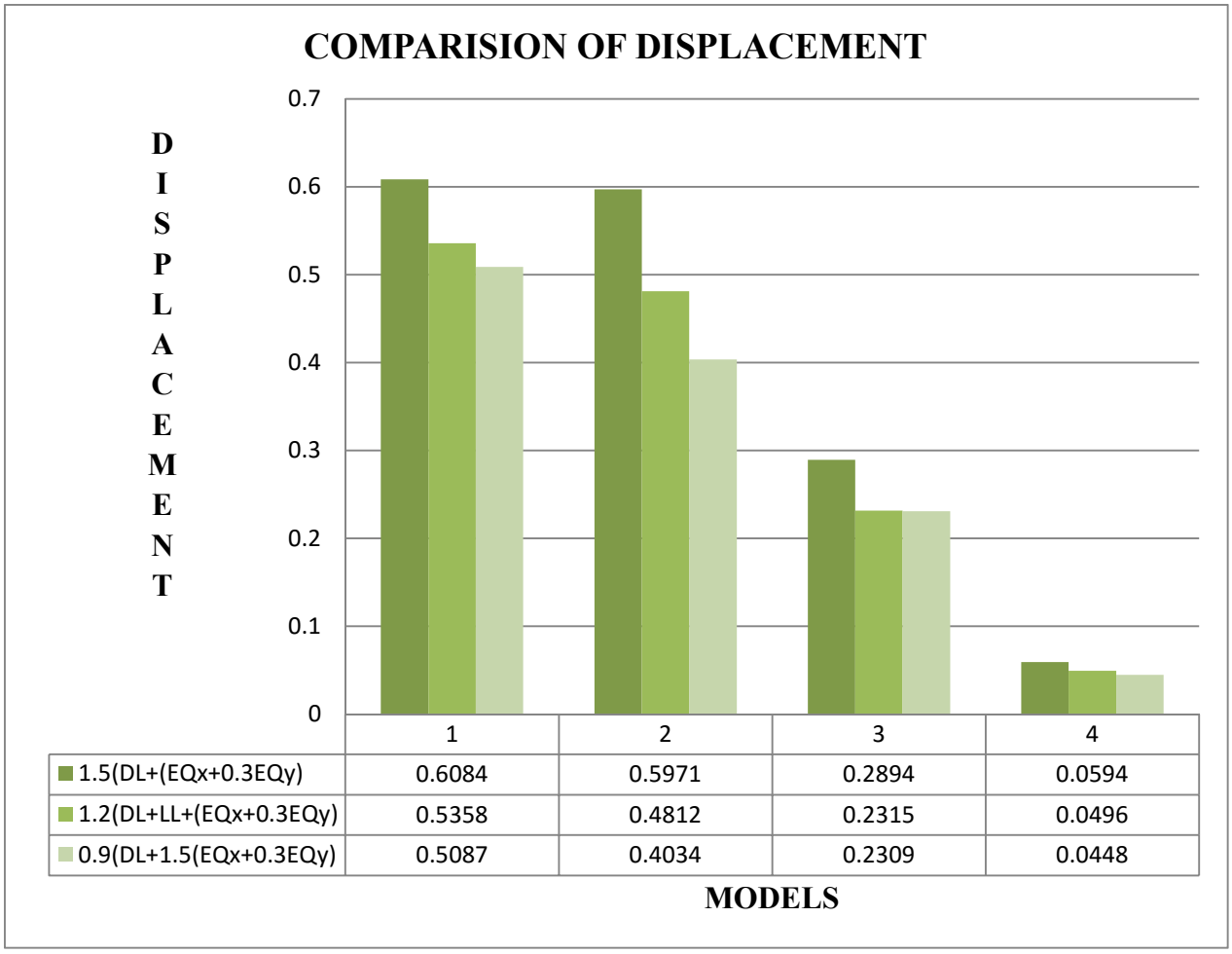

Figure 40: Comparison of Maximum Displacement for all models

Figure 40 shows comparison of maximum displacement for all four models. Here in this figure 40 model 1 (without stiffness in expansion joint) has maximum displacement of 0.6084 m. Model 2 (lead rubber bearing in expansion joint) has maximum displacement of 0.5971m which is less than model 1. Model 3 (rubber isolator in expansion joint) has maximum displacement of 0.2894m which is less as compare to model 1 and model 2. Model 4 (high damping rubber bearing in expansion joint) has maximum displacement of 0.0594m which is very less as compare to all three load cases. So from the comparison of maximum displacement we obtain that high damping rubber bearing has very high resistance to pounding force and can be used in expansion joint for future design.

Chapter 6
CONCLUSION

6.1 General

This chapter of thesis provides the conclusion of all the work done for pounding control design of elevated bridge. Here in this thesis we modelled a bridge using CSI Bridge software. Then we provide bearing at expansion joint location. Then response spectrum analysis of bridge was done. All the results were recoded and comparison for maximum value of results had done to find best bearing at expansion joint to overcome pounding in bridge.

6.2 Conclusion

In this thesis we analyse a bridge to see the effects of pounding. Then we provide bearing at expansion joint to overcome pounding. The following conclusions are given below.

1. From comparison of maximum axial force we find that maximum axial force was large in load case 1 for all the four models. Model 1 (without stiffness in expansion) was more critical for pounding. Maximum axial force was much larger in model1 as compare to all other models. When we provide lead rubber bearing in expansion joint in model 2 there was decrease in maximum axial force. But it was more than model 3 and 4. In model 3 we provide rubber isolator in expansion joint. In model 4 we provide high damping rubber bearing whose performance was much better than all other three models.
2. From comparison of maximum moment we find that maximum moment was much higher in model 1. After providing lead rubber bearing and rubber isolator in model 2 and 3 maximum moment decreases due to their high effective stiffness. Model 4 had high effective stiffness than other three models.so the value of maximum moment was much less.
3. From the comparison of maximum stress at top and bottom of bridge model 4 (high damping rubber bearing in expansion joint) performs better than other three models under seismic excitation.
4. From the comparison of maximum displacement and bottom of bridge model 4 (high damping rubber bearing in expansion joint) performs better than other three models under seismic excitation.

5. So by providing high stiffness bearing like High Damping Rubber bearing at expansion joint we can control pounding in bridge.

6.3 Future scope

1. To analyse the bridge under non-linear time history analysis.
2. To analyse the bridge considering soil structure interaction at piers of bridge.
3. To analyse the damaged bridge structure after applying retrofitting techniques to check the serviceability conditions.

REFRENCES

[1] Amjadian, M., & Agrawal, A. K. (2016). Rigid-body motion of horizontally curved bridges subjected to earthquake-induced pounding, "*Journal of Bridge Engineering"*, *21*(12), 04016090.

[2] Won, J. H., Mha, H. S., & Kim, S. H. (2015). Effects of the earthquake-induced pounding upon pier motions in the multi-span simply supported steel girder bridge, "*Engineering Structures"*, *93*, 1-12.

[3] Shrestha, B., Hao, H., & Bi, K. (2014). Effectiveness of using rubber bumper and restrainer on mitigating pounding and unseating damage of bridge structures subjected to spatially varying ground motions, "*Engineering Structures"*, *79*, 195-210.

[4] Huo, Y., & Zhang, J. (2012). Effects of pounding and skewness on seismic responses of typical multispan highway bridges using the fragility function method, "*Journal of Bridge Engineering"*, *18*(6), 499-515.

[5] Dimitrakopoulos, E. G. (2011). Seismic response analysis of skew bridges with pounding deck–abutment joints, "*Engineering Structures"*, *33*(3), 813-826.

[6] Wang, T. L., & Li, Q. N. (2011, April). Effect of expansion joint on seismic response of curved ramp bridge, "In *Electric Technology and Civil Engineering (ICETCE), 2011 International Conference on"* (pp. 5904-5907). IEEE.

[7] Meng, Q., & Xia, Y. (2011, June). Seismic pounding effect in bridges with high piers, In "*Remote Sensing, Environment and Transportation Engineering (RSETE), 2011 International Conference" on* (pp. 3455-3460). IEEE.

[8] Wang, J. W., Li, J. Z., & Fan, L. C. (2007). Current Studies on Seismic Pounding Effect between Adjacent Bridge Decks and Falling-off Prevention Measures, "*Journal of Highway and Transportation Research and Development" (English Edition)*, *2*(2), 52-58.

[9] Soyluk, K. (2004). Comparison of random vibration methods for multi-support seismic excitation analysis of long-span bridges", "*Engineering Structures*, *26*(11), 1573-1583.

[10] Kim, S. H., & Shinozuka, M. (2003). Effects of seismically induced pounding at expansion joints of concrete bridges, "*Journal of engineering mechanics"*, *129*(11), 1225-1234.

[11] DesRoches, R., & Muthukumar, S. (2002). Effect of pounding and restrainers on seismic response of multiple-frame bridges".,"*Journal of Structural Engineering*, *128*(7), 860-869.

[12] Jankowski, R., Wilde, K., & Fujino, Y. (2000). Reduction of pounding effects in elevated bridges during earthquakes, "*Earthquake engineering & structural dynamics"*, *29*(2), 195-212.

[13] Kim, S. H., Lee, S. W., Won, J. H., & Mha, H. S. (2000). Dynamic behaviors of bridges under seismic excitations with pounding between adjacent girders, "In *Proc., 12th World Conf. on Earthquake Engineering"*.

[14] Jankowski, R., Wilde, K., & Fujino, Y. (1998). Pounding of superstructure segments in isolated elevated bridge during earthquakes, "*Earthquake engineering & structural dynamics"*, *27*(5), 487-502.
[15] Malhotra, P. K. (1998). Dynamics of seismic pounding at expansion joints of concrete bridges", "*Journal of Engineering Mechanics*, *124*(7), 794-802.
[16] Indian Standard, I. S. (2002). Indian Standard, Criteria for earthquake resistance design of structures, Fifth Revision, Part-I "*Bureau of Indian Standard", New Delhi*.
[17] Congress, I. R. (2010). IRC-6: 2010 Standard Specifications and Code of Practice for Road Bridges Section: II Loads and Stresses.
[18] CSI Bridge software

JAYPEE UNIVERSITY OF INFORMATION TECHNOLOGY, WAKNAGHAT
LEARNING RESOURCE CENTER

PLAGIARISM VERIFICATION REPORT

Date: 11/05/2018

Type of Document (Tick): Thesis | M.Tech Dissertation/ Report ✓ | B.Tech Project Report | Paper

Name: ROHIT SHARMA Department: Civil Engg. (SE)

Enrolment No. 162663 Registration No. _____

Phone No. 9816998150 Email ID. imrohitsharma@gmail.com

Name of the Supervisor: Mr. Chandra Pal Gautam

Title of the Thesis/Dissertation/Project Report/Paper (In Capital letters):

POUNDING CONTROL DESIGN OF ELEVATED BRIDGES UNDER SEISMIC EXICATION

Kindly allow me to avail Turnitin software report for the document mentioned above.

Rohit Sharma
(Signature)

FOR ACCOUNTS DEPARTMENT:

Amount deposited: Rs. <20/- Dated: 11/5/18 BRN1805/318 Receipt No. .....
(Enclosed payment slip)

(Account Officer)

FOR LRC USE:
The above document was scanned for plagiarism check. The outcome of the same is reported below:

Copy Received on	Report delivered on	Similarity Index in %	Submission Details	
11/05/2018	11/05/2018	12%	Word Counts	20,476
			Character Counts	89,155
			Page counts	82
			File Size	7.27MB

Checked by
Name & Signature

Librarian

LIBRARIAN
LEARNING RESOURCE CENTER
Jaypee University of Information Technology
Waknaghat, Distt. Solan (Himachal Pradesh)
Pin Code: 173234

turnitin

Digital Receipt

This receipt acknowledges that Turnitin received your paper. Below you will find the receipt information regarding your submission.

The first page of your submissions is displayed below.

Submission author:	Rohit. Sharma
Assignment title:	MTech Project Reports
Submission title:	POUNDING CONTROL DESIGN OF...
File name:	M.Tech_Rohit_162663.pdf
File size:	7.27M
Page count:	82
Word count:	20,476
Character count:	89,155
Submission date:	11-May-2018 04:49PM (UTC+0530)
Submission ID:	962363755

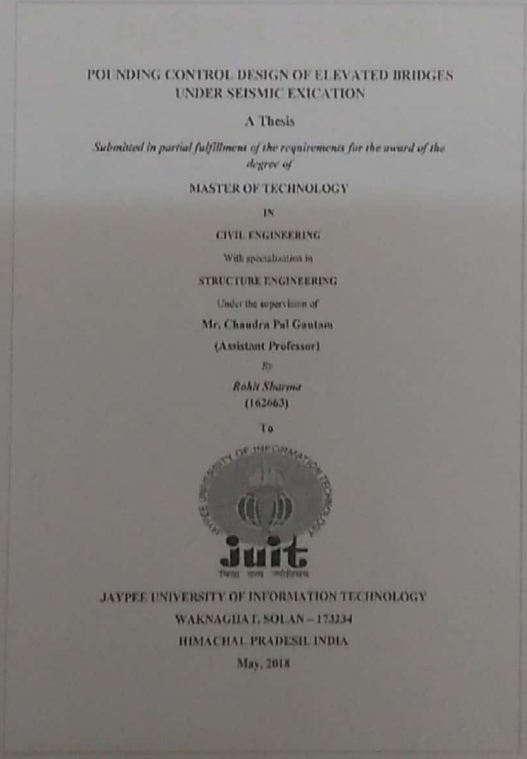

POUNDING CONTROL DESIGN OF ELEVATED BRIDGES UNDER SEISMIC EXICATION

A Thesis

Submitted in partial fulfillment of the requirements for the award of the degree of

MASTER OF TECHNOLOGY

IN

CIVIL ENGINEERING

With specialization in

STRUCTURE ENGINEERING

Under the supervision of

Mr. Chandra Pal Gautam

(Assistant Professor)

By

Rohit Sharma

(162663)

To

JAYPEE UNIVERSITY OF INFORMATION TECHNOLOGY

WAKNAGHAT, SOLAN – 173234

HIMACHAL PRADESH, INDIA

May, 2018